JOINT TRANSPORTATION
RESEARCH PROGRAM
INDIANA DEPARTMENT OF TRANSPORTATION
AND PURDUE UNIVERSITY

Link Slab Details and Materials

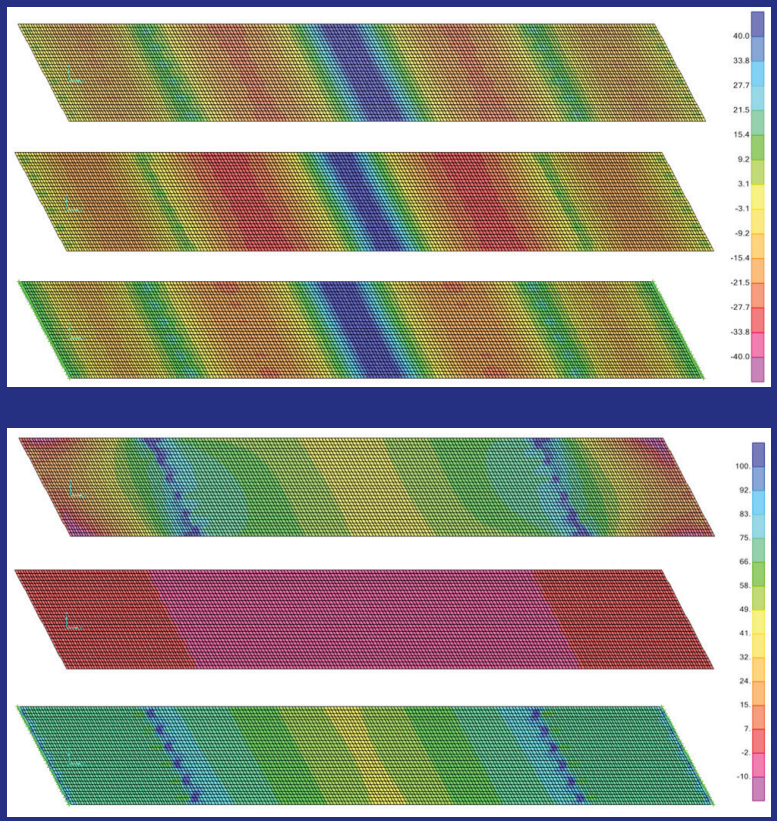

Ghadir Haikal, Julio A. Ramirez, Mohammad R. Jahanshahi,
Sandra Villamizar, Osama Abdelaleim

SPR-4223 • Report Number: FHWA/IN/JTRP-2019/10 • DOI: 10.5703/1288284316920

RECOMMENDED CITATION

Haikal, G., Ramirez, J. A., Jahanshahi, M. R., Villamizar, S., & Abdelaleim, O. (2019). *Link slab details and materials* (Joint Transportation Research Program Publication No. FHWA/IN/JTRP-2019/10). West Lafayette, IN: Purdue University. https://doi.org/10.5703/1288284316920

AUTHORS

Ghadir Haikal, PhD
Assistant Professor of Civil Engineering
Lyles School of Civil Engineering
Purdue University

Julio A. Ramirez, PhD
Kettelhut Professor of Civil Engineering
Lyles School of Civil Engineering
Purdue University

Mohammad R. Jahanshahi, PhD
Assistant Professor of Civil Engineering
Lyles School of Civil Engineering
Purdue University

Sandra Villamizar
Osama Abdelaleim
Graduate Research Assistants
Lyles School of Civil Engineering
Purdue University

ACKNOWLEDGMENTS

The authors acknowledge the participation of the members of the Study Advisory Committee. Their support and assistance is appreciated.

JOINT TRANSPORTATION RESEARCH PROGRAM

The Joint Transportation Research Program serves as a vehicle for INDOT collaboration with higher education institutions and industry in Indiana to facilitate innovation that results in continuous improvement in the planning, design, construction, operation, management and economic efficiency of the Indiana transportation infrastructure. https://engineering.purdue.edu/JTRP/index_html

Published reports of the Joint Transportation Research Program are available at http://docs.lib.purdue.edu/jtrp/.

NOTICE

TECHNICAL REPORT DOCUMENTATION PAGE

1. Report No. FHWA/IN/JTRP-2019/10	**2. Government Accession No.**	**3. Recipient's Catalog No.**
4. Title and Subtitle Link Slab Details and Materials		**5. Report Date** May 2019 **6. Performing Organization Code**
7. Author(s) Ghadir Haikal, Julio A. Ramirez, Mohammad R. Jahanshahi, Sandra Villamizar, and Osama Abdelaleim		**8. Performing Organization Report No.** FHWA/IN/JTRP-2019/10
9. Performing Organization Name and Address Joint Transportation Research Program Hall for Discovery and Learning Research (DLR), Suite 204 207 S. Martin Jischke Drive West Lafayette, IN 47907		**10. Work Unit No.** **11. Contract or Grant No.** SPR-4223
12. Sponsoring Agency Name and Address Indiana Department of Transportation (SPR) State Office Building 100 North Senate Avenue Indianapolis, IN 46204		**13. Type of Report and Period Covered** Final Report **14. Sponsoring Agency Code**

15. Supplementary Notes

Conducted in cooperation with the U.S. Department of Transportation, Federal Highway Administration.

16. Abstract

This report contains the findings of a synthesis study on the use of link slabs to eliminate intermediate joints in bridges of Indiana. The study was conducted under the sponsorship of the Joint Transportation Research Program. The motivation for the study was to investigate this promising technique to mitigate the damage associated with expansion joints that has long been recognized as a persistent and costly issue negatively impacting the bridge service life.

The report summarizes the background information and motivation for the study. It also provides a description of the report organization. The results of an extensive literature review of DOTs' experience related to the use of this system and main research findings are presented as well as construction practice and examples of application. The results of the analysis of a bridge in Indiana where the link slab system has been implemented are presented. The bridge connecting the State Road 68 over the Interstate 64 was selected as a representative bridge based on the analysis of the inspection.

A parametric study on the effects of various parameters was conducted to evaluate the effect of support conditions and debonded length on the stress distribution and potential crack initiation in link slabs. Each variable was investigated separately to isolate its effect. Two bridge structures were investigated in this study. The first structure (Case 1) represents a bridge structure rehabilitated using link slabs. A second bridge structure (Case 2) with the same geometrical and material properties, but with a continuous and fully bonded deck, was also included in the parametric study for comparison purposes. This structure simulated new bridge construction.

17. Key Words bridge, concrete, fiber, performance, detailing, temperature effects, link slab, jointless bridges, bridge deck joints replacement, literature review, finite element	**18. Distribution Statement** No restrictions. This document is available through the National Technical Information Service, Springfield, VA 22161.

19. Security Classif. (of this report) Unclassified	**20. Security Classif. (of this page)** Unclassified	**21. No. of Pages** 94	**22. Price**

Executive Summary

This report contains the findings of a synthesis study on the use of link slabs to eliminate intermediate joints in bridges of Indiana. The study was conducted under the sponsorship of the Joint Transportation Research Program. The motivation for the study was to investigate this promising technique to mitigate the damage associated with expansion joints that has long been recognized as a persistent and costly issue negatively impacting the bridge service life.

The report consists of five chapters. The first chapter summarizes the background information and motivation for the study. It also provides a description of the report organization. In Chapter 2, the results of an extensive literature review of DOT experiences, including Indiana's, with the use of this system, design and construction practices are summarized as well. An extensive review of the research on these systems is also summarized in Chapter 2. The results of the analysis of a bridge in Indiana where the link slab system has been implemented are summarized in Chapter 3. A comparative numerical study is conducted on the bridge between the models representing the bridge before and after the link slab construction under live and thermal loads. In Chapter 4, a parametric study is conducted to evaluate the effect of support conditions and debonded length on the stress distribution and potential crack initiation in link slabs using a two-span bridge model. The goal of the parametric study is to compare the performance of fully bonded link slabs, as implemented in Indiana, with the more common debonded link slabs as recommended in the literature.

The main findings, conclusions and recommendations for implementation and further research from the study are given in Chapter 5. Major findings include limitations of current design approaches, the effect of support conditions, and observed cracking issues, in particular, in Indiana where the design detail used lacks a debonded zone. For improved performance, suggestions in the literature include the use of high tensile materials and improved details, such as the debonded slab with an additional transition zone between the link slab and the existing deck. However, these improvements would not eliminate cracking unless thermal effects are addressed. Numerical analyses in Chapter 3 show that these loads are major contributors to high stresses in the deck leading to observed cracks in the field. Further investigation is needed to examine the appropriate method for considering temperature effects and support conditions in the design of link slabs.

Contents

1. Introduction 1
1.1 Background 1
1.2 Problem Statement 2
1.3 Objectives and Scope 3
1.4 Information Collection 4
1.5 Report Organization 4

2. Literature Review 7
2.1 DOT Experience 7
2.2 Previous Research on Link Slabs 8
2.2.1 North Carolina Department of Transportation (NCDOT) 8
2.2.2 Michigan Department of Transportation (MDOT) 15
2.2.3 Virginia Department of Transportation (VDOT) 19
2.2.4 New York State Department of Transportation (NYSDOT) 20
2.2.5 Hawaii Department of Transportation (HDOT) 21
2.2.6 Louisiana Department of Transportation (LaDOTD) 23
2.2.7 Ministry of Transportation of Ontario (MTO) 24
2.3 Design Specifications and State Construction Practices 25
2.4 Assessment of Existing Indiana Link Slab Bridges 31
2.4.1 I-64 EB/WB over Captain Frank Road 32
2.4.2 SR 64 over SR 37 33
2.4.3 Owensville Road over I-64 34
2.4.4 SR-68 over I-64 35
2.4.5 Hillcrest Road over US-50 36
2.4.6 Summary of Inspection Reports 37

2.5 Summary of the Literature and Practice Review . . . 39

3. Numerical Analysis of Indiana Bridge . . . 43
3.1 Bridge Model . . . 43
3.1.1 Geometry and Boundary Conditions . . . 43
3.1.2 Loading . . . 46
3.2 Results . . . 48
3.3 Parametric Study . . . 50
3.3.1 Effect of Material . . . 51
3.3.2 Effect of Boundary Conditions . . . 52

4. Bridge Parameter Investigation . . . 55
4.1 Effect of Support Conditions . . . 58
4.2 Effect of Debonded Length . . . 60
4.3 Conclusions of Parametric Study . . . 64

5. Findings, Conclusions, and Proposed Recommendations for Implementation . . . 65
5.1 Summary . . . 65
5.2 Findings . . . 65
5.2.1 Literature Review . . . 65
5.2.2 Analysis of Indiana Bridge . . . 70
5.2.3 Bridge Parameter Investigation . . . 71
5.3 Conclusions . . . 72
5.3.1 Use by DOTs . . . 72
5.3.2 Design Practice . . . 73
5.3.3 Research . . . 73
5.4 Recommendations for Implementation . . . 74
5.5 Suggestions for Future Research . . . 75

References . . . 77

List of Figures

1.1 Deck joint replacement approach with link slabs 2

2.1 Debonded link slab configuration tested by Caner and Zia [1998] 12
2.2 Link slab detail [Wing and Kowalsky, 2005] 14
2.3 ECC link slab configuration proposed by Li et al. [2003] 16
2.4 Link slab detail used in Michigan [Aktan et al., 2008] 18
2.5 UHPC link slab detail [Graybeal, 2014] 21
2.6 HPFRCC precast link slab tested by Reyes and Robertson [2011] 22
2.7 GFRP link slab detail 23
2.8 Full-scale beam testing setup as presented by Li and Saber [2009] 23
2.9 Link slab details used in Canada [Lam et al., 2008] 25
2.10 VDOT link slab detail [VDOT, 2018] 28
2.11 NYSDOT link slab detail [NYSDOT, 2018] 29
2.12 Location of the existing link slab bridges 31
2.13 Link slab detail (I-64 over Captain Frank) 33
2.14 Link slab detail (SR 64 over SR 37) 34
2.15 Link slab detail (Owensville Road over I-64) 35
2.16 Link slab detail (SR 68 over I-64) 36
2.17 Link slab detail (Hillcrest Road over US-50) 37
2.18 Cracking in Indiana link slab bridges as reported in inspection reports 38

3.1 Bridge elevation and cross-section as reported in drawings 44
3.2 Plan view of the girders and diaphragms of the bridge model 44
3.3 Boundary conditions for the concrete girders on the left and the steel girders on the right 45
3.4 Applied (dashed) and AASHTO (solid) Gradient temperature diagrams for concrete and steel structures 47

3.5 Axial forces (kips) in the slab due to fully loaded structure under live load. The top figure is the bridge with expansion joint. The bottom figure is the bridge with link slabs . . . 48
3.6 Axial forces (kips) in the slab due to uniform increase in temperature. The top figure is the bridge with expansion joint. The bottom figure is the bridge with link slabs . . . 49
3.7 Axial forces (kips) in the slab due to uniform decrease in temperature. The top figure is the bridge with expansion joint. The bottom figure is the bridge with link slabs . . . 49
3.8 Axial forces (kips) in the slab due to gradient temperature. The top figure is the bridge with expansion joint. The bottom figure is the bridge with link slabs . . . 50
3.9 Plan view of the girders and diaphragms of the bridge model where all girders are made of concrete . . . 51
3.10 Axial forces (kips) in the slab due to uniform decrease in temperature. The top figure is the original bridge with link slab. The bottom figure is the bridge variant (All concrete girders) with link slab . . . 52
3.11 Axial forces (kips) in the slab due to fully loaded structure under live load. The top figure is the bridge with HHRHRHH support configuration. The middle figure is the bridge with RRRHRRR support configuration. The bottom figure is the bridge with RRRHRRR support configuration and supports representing approach slab . . . 53
3.12 Axial forces (kips) in the slab due to fully loaded structure under live load. The top figure is the bridge with HHRHRHH support configuration. The middle figure is the bridge with RRRHRRR support configuration. The bottom figure is the bridge with RRRHRRR support configuration and supports representing approach slab . . . 54

4.1 Bridge deck link slab (Case 1) . . . 56
4.2 Continuous bridge deck (Case 2) . . . 56
4.3 Tie constraint locations . . . 57
4.4 Model assembly for live load . . . 57
4.5 Effect of boundary conditions under live load . . . 59
4.6 Effect of boundary conditions under uniform temperature load . . . 59
4.7 Effect of debonding under live load for support conditions: RHHR; FFRH; HHHH; and HRHH . . . 61
4.8 Effect of debonding under live load for support conditions: HRRH; HRRR; and RRHR . . . 62
4.9 Effect of debonding under uniform temperature load for support conditions: RHHR; FFRH; HHHH; and HRHH . . . 63

4.10 Effect of debonding under uniform temperature load for support conditions: HRRH; HRRR; and RRHR 64

5.1 ECC link slab configuration proposed by Li et al. [2003] 75

List of Tables

1.1 Contacted state agencies 4

2.1 Link slab applications 8
2.2 Summary of state practices 30
2.3 Summary of geometric properties of Indiana link slab bridges 32
2.4 Summary of inspection reports of Indiana link slab bridges 32
2.5 Literature summary 39
2.6 Mix proportions 41
2.7 Properties of GFRP reinforcement 41

3.1 Mesh dimensions for concrete and steel structures 46

4.1 FEM material properties 55
4.2 Surfaces for tie constraint definition 57
4.3 Maximum stresses at top of link slab due to live load 60
4.4 Maximum stresses at top of link slab due to uniform temperature load 60

Chapter 1

Introduction

1.1 Background

Conventional multispan bridges have expansion joints usually placed at the end of the spans over the piers and the abutments. The joints are designed to allow superstructure movement caused by shrinkage, creep, and thermal effects. The damage associated with expansion joints has long been recognized as a persistent and costly issue that can negatively impact the bridge service life [Alampalli and Yannotti, 1998; Au et al., 2013]. Bridge deck joints allow the entrance of corrosive chemicals and debris causing premature deterioration of concrete bridge decks, beam-ends, girder bearings, and supporting substructure [Kim et al., 2004].

The United States Federal Highway Administration (FHWA) and individual state departments of transportation (DOTs) are actively promoting the implementation of jointless bridges, i.e., bridges without expansion joints, to address the durability problems and poor performance of deck joints. Jointless bridges have been used in many states. The elimination of deck joints results in additional forces that need to be considered in the design of the bridge systems. Bridge deck joints can be replaced at the abutments by using an integral abutment, semi-integral abutment, or deck extension. At piers, joint elimination can be achieved by using continuous-for-live-load bridge structures or by installing **link slabs**.

Link slabs are typically used by DOTs for replacing deck expansion joints over piers in short and medium multispan bridges (i.e., span length from 30 ft to 100 ft). A link slab is the portion of the deck over the joint that connects two adjacent deck spans, integrating the deck as a fully continuous system while the girders remain simply-supported [Caner and Zia, 1998]. Link Slabs can be implemented in concrete and steel beam bridge superstructure. The primary purpose of making the deck continuous is to avoid span separation and deterioration due to leaking [Caner et al., 2002; Sevgili and Caner, 2009]. Fig. 1.1 shows the deck joint

replacement approach using link slabs.

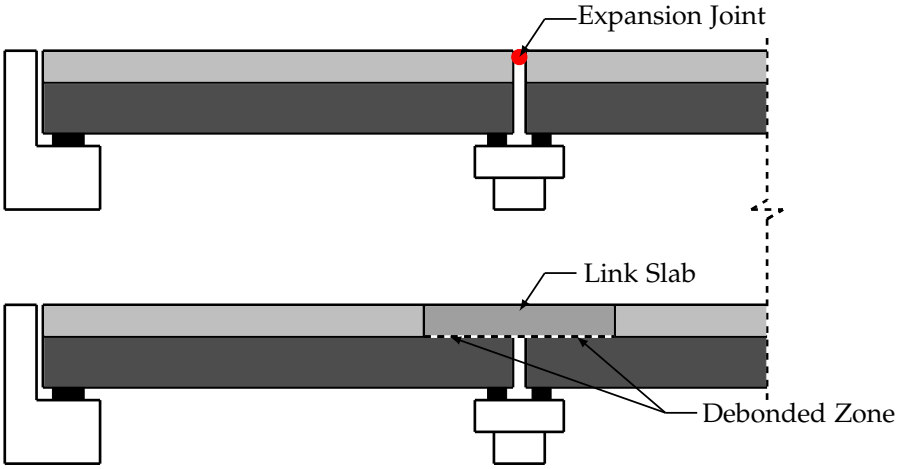

Figure 1.1: Deck joint replacement approach with link slabs

The majority of DoTs in the United States and Canada provide a debonded zone at each adjacent bridge span where composite action does not exist between the link slab and girder ends, as illustrated in Fig. 1.1. This debonded zone is used to reduce the stiffness and stresses in the connection. It is achieved by removing any structural mechanism capable of transferring load (e.g., stirrups and shear stud connectors) and by placing a bond breaker material between the beam and the deck. However, there are some exceptions as the state of Indiana, where this debonding is not provided. The absence of a debonded zone, as well as the substantial cracking observed in existing link slabs in Indiana, motivated the numerical investigation conducted in this study.

1.2 Problem Statement

Link slabs offer the potential to reduce maintenance costs and allow the use of prefabricated bridge element systems (PBES) without requiring the casting of integral end diaphragms [Culmo et al., 2017]. They improve riding surface as well as extend the bridge service life at a fraction of cost and construction-caused downtime compared to other existing methods for replacing joints. However, cracking in link slabs has been a recurring issue reported by inspectors, which in severe cases leads to leaking and deterioration of the bridges as well [Aktan et al., 2008; Li et al., 2005, 2008]. Once water leaks through the cracks carried deicing salts lead to accelerated deterioration of the deck, superstructure, and substructure. Consequently, the deteriorated bridge structure will require to be replaced before its design life, negating the above-mentioned cost-effective advantages of link slabs.

Different solutions have been proposed to address the cracking issue in link slabs. Some researchers attribute the cracking to shrinkage and temperature gradients. As a result, several studies have been focusing on new material designs with improved tensile strength [Li et al., 2003; Ozyildirim et al., 2017; Hoomes et al., 2017]. Other researchers attribute the cracks to the tension force resulted from continuity moments, poor construction practices, and improper detailing for the adequate accommodation of the bridge superstructure movement [Aktan et al., 2008; Li et al., 2003; Ulku et al., 2009; Okeil and El-Safty, 2005]. To this end, alternative design procedures and joint details have been developed.

1.3 Objectives and Scope

This research focuses on reviewing the current state-of-the-art and state-of-the-practice related to link slabs in bridge decks. Information is collected and reported about materials, design provisions, construction procedures, system performance, and design details that have been studied for use or that are still being used in the United States and other countries. The goal is to provide a better understanding of the behavior of link-slab bridges and elucidate the most practical and efficient practices. The following tasks were identified to achieve the project objectives:

Task 1 — Review of relevant literature, findings of previous investigations, existing design methods, domestic and foreign specifications, field implementations, and other sources that help to establish the state of knowledge on link slabs.

Task 2 — Summarize available information on the design and construction of link slabs in bridge decks.

Task 3 — Assess qualitatively the existing link-slabs bridges in the state of Indiana to identify potential factors and conditions affecting the behavior of link slabs as well as detailing and materials used.

Task 4 — Examine current construction practices to obtain a comprehensive understanding of the existing retrofitting methods for bridges where link slabs are used to replace joints and compared with evidence from performance wherever available as well as to ease of construction.

Task 5 — Identify critical parameters that affect the behavior of link slabs and research areas of improvement.

Task 6 — Perform preliminary finite element analysis to investigate the role played by debonding and examine other potential parameters that influence the behavior of link slabs used in the state of Indiana. This task was added during project progress, motivated by observations made during the bridge assessment (Task 3), where substantial deterioration was noted in existing link slabs.

Task 7 — Submit a final report that summarizes the entire research project and provides suggestions for future research needs.

1.4 Information Collection

Information is collected through a review of existing literature on the design, implementation, and inspection of link slab joints. The review is limited to available versions of state bridge specifications, manuals, guidelines, and standard drawings from DOTs in which the link slabs have been implemented. In the review of the specs, explicit provisions related to the design of link slabs are identified. Technical information is collected from research projects, field implementations, and past surveys conducted by different DOTs or any other institute. Six state agencies were contacted, with the assistance of the Indiana Department of Transportation (INDOT) personnel, four which responded (Table 1.1). All the documents referred in this synthesis come from published sources.

Table 1.1: Contacted state agencies

Agency	Contact Person	E-mail	Response
CME Associates	Mike Culmo	culmo@cmeengineering.com	Yes
Michigan	Matt Chynoweth	ChynowethM@michigan.gov	Yes
North Carolina	Daniel Muller	dmuller@ncdot.gov	No
Virginia	Jeffrey Milton	Jeffrey.Milton@VirginiaDOT.gov	Yes
New York	Brenda Crudele	brenda.crudele.@dot.ny.gov	Yes
Massachusetts	Alexander Bardow	alexander.bardow@state.ma.us	No

1.5 Report Organization

The report is organized in five chapters. Chapter 1 provides the background information and problem statement for the research project and describes the research objectives and methodology used for information gathering. Chapter 2 summarizes the findings of the literature review and presents the identified knowledge gaps. Chapter 3 summarizes the numerical

investigation performed on an existing bridge in Indiana. Chapter 4 shows the results of a preliminary parameter investigation conducted to evaluate the effect of support conditions and debonded length on the behavior of link slabs. Chapter 5 presents the conclusions and provides recommendations for further research.

Chapter 2

Literature Review

This chapter summarizes the information gathered from a review of literature performed to establish the state of knowledge on link slabs. Specific areas of interest regarding link slabs include (1) review of design and construction practices with potential to enhance the performance, (2) lessons learned, (3) material specifications, and (4) factors that affect the behavior.

2.1 DOT Experience

The review of available information from DOTs conducted in this project indicated that around 30% of them in the United States had experience with the link slabs applications. The information is summarized in Table 2.1 in the categories of research, field work, and specifications. Approximately two-thirds of the reported agencies have performed research or implemented the link-slab system in the field. Nearly one-third of them provided design provisions or official details. North Carolina, Michigan, Virginia, and New York were identified as key DOTs that use link slabs. Many bridges have been retrofitted using link slabs in these states. Notice in Table 2.1 that some state highway agencies were contacted and provided information.

Table 2.1: Link slab applications

State	Research	Field Work	Specifications
Delaware	NA	Yes	NA
Florida	Yes	NA	Yes
Georgia	Yes	NA	NA
Hawaii	Yes	NA	NA
Indiana	NA	Yes	NA
Iowa	Yes	NA	NA
Massachusetts[a]	NA	Yes	Yes
Michigan[b]	Yes	Yes	NA
Missouri	NA	Yes	NA
Nebrasca	Yes	NA	NA
New York[b]	Yes	Yes	Yes
North Carolina	Yes	Yes	Yes
Tennessee	NA	Yes	NA
Utah	NA	NA	Yes
Virginia[b]	Yes	Yes	Yes

Note: NA = Not Available.
Information provided by:
[a] CME Associates
[b] State highway agency contacted.

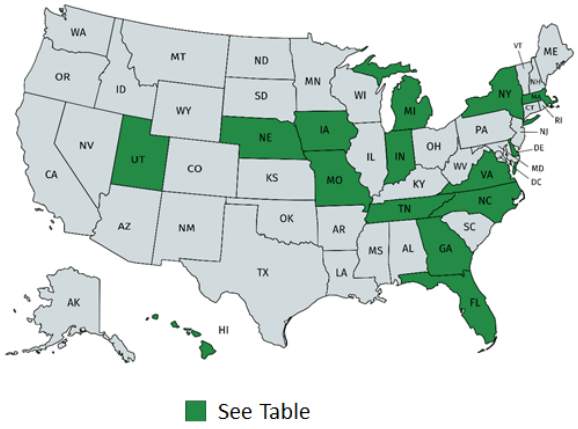

2.2 Previous Research on Link Slabs

2.2.1 North Carolina Department of Transportation (NCDOT)

2.2.1.1 Gastal

Gastal [1986] developed analytical models to investigate the elastic and inelastic response and strength of jointless bridge decks. The numerical approach involved isoparametric beam elements to represent the cross-sectional and material properties of the girders and deck. The full-depth link slab was modeled through a uniaxial spring element located at the centroidal line of the deck that had the same length as the spacing between the ends of adjacent girders. The bearing supports were idealized as uniaxial springs attached to the respective nodal points. The finite element model of the bridge was validated against analytical and experimental data on simply-supported and continuous beams reported in the literature.

Gastal [1986] applied the analytical approach on the solution of two design problems with bridge jointless decks. The first problem corresponded to a 100 ft steel-girder bridge with two equal spans. The superstructure consisted of W33 x 118 girders supporting a 7 ft by 7 in concrete deck slab. The second problem consisted of a 264 ft precast, prestressed girder bridge with four equal spans of 66 ft each. The superstructure consisted of AASHTO Type IV girders supporting a 6 ft by 6 in reinforced concrete deck slab. The concrete compressive strength of the deck and the girders were 3500 psi and 6000 psi, respectively. Gastal [1986] compared different construction details in the analysis such as fully-continuous, only deck

continuous, and non-continuous. Shored and unshored deck construction was also examined. Several loadings were considered in the analysis including prestressing, dead loads, live loads, support displacements, temperature, and time-dependent effects. All the external loads were applied using both load increment and displacement increment methods. The support arrangements were varied by changing the position of the hinged (H), and roller (R) supports at each end of the girder. The five support configurations evaluated were: RHHR; HRRH; HRHR; HRRR; and RRRR. The effects of temperature were evaluated by considering two temperature variation gradients under the action of the same service live load. A constant temperature variation across the depth of the superstructure of 50 °F was assumed to model a seasonal temperature. A linearly decreasing gradient ranging from 50 ° to 0 °F was used for a daily variation of temperature.

Based on the study, it was concluded that the behavior of the jointless deck-continuous beams was significantly influenced by the girder support conditions. The deck connection over the intermediate support was, under any applied load, subjected to bending and axial force. Depending on the type and arrangement of the supporting conditions, tension or compression can occur at the deck connection, producing a different behavior of the whole structure for each supporting situation. The support arrangements HRHR, HRRR, and RRRR behaved quite similarly to a non-continuous beam but with slightly smaller deflections and much less ductility. For these cases, the maximum capacity of the link slab was governed by the yield of the reinforcing steel (assumed at a limiting strain of 1%). For the support arrangement HRRH, the deck behaved quite similarly to a non-continuous beam. A compressive force was encountered at the deck connection which yields a much lower moment carrying capacity and ductility, allowing failure to occur by crushing of concrete at the bottom face of the deck. For the RHHR case, the deflections at the service load range became comparable to those of a fully-continuous beam. Failure was obtained by extensive yielding of the reinforcing steel at the connection, and its ultimate load capacity was well above that of a non-continuous beam. The researchers noted that temperature gradients and time effects on the concrete from creep and shrinkage did not show significant differences in deflections and cracking from those observed by having fully-continuous and non-continuous beams. Their long-term strength was also unchanged. In addition, the authors recommended increasing the length of the deck connections to achieve more flexibility, either by enlarging the gap space between girders or by providing some unbonded distance between deck and beams at each side of the support.

2.2.1.2 El-Safty

El-Safty [1994] updated the work accomplished by Gastal [1986] to account for partial debonding of the deck from the girder ends. The link slab was made longer than the space between the two adjacent girders by breaking the composite action between the deck and the girder

for a certain distance. The length of this debonded zone varied from 1% to 8% of each adjacent span length. The link slab was modeled as a spring element with only axial stiffness. The length of the connection spring element was measured between its contact points with the girders. The flexural stiffness of the deck was neglected at the connection element; A rotational restriction to the spring element was provided due to its offset position from the centroid of the composite section. Both concrete deck and the girders were modeled using isoparametric beam elements. The bearing supports were modeled with uniaxial spring elements attached to the respective nodal points.

El-Safty [1994] considered two set of problems related to multi-span girders with jointless bridge deck to validate the analytical model. The first problem was a steel superstructure bridge with two equal spans of 20 ft. The superstructure consisted of W12x26 girders supporting a 4 in thick and 2 ft wide concrete deck slab. The spacing at the joint was 4 in. The second problem corresponded to the same four-span prestressed girder bridge analyzed by Gastal [1986]. Four construction details were studied under this study: fully-continuous, non-continuous, only deck-continuous, and partially debonded continuous deck. The four boundary conditions considered were RRRR, RHRH, RHHR, and HRRH. Different loadings were prestressing, dead loads, live loads, support displacements, temperature, and time-dependent effects. Symmetrical and unsymmetrical loading conditions were examined for each support arrangement. Thermal effects were analyzed considering a given temperature distribution over the composite cross-section. The temperature distribution was assumed to be stationary in time and non-variable along the member length.

The study showed that boundary conditions and loading arrangement significantly affect the responses of the deck with a partially debonded connection. For beams supported by two bearing pads, one at each side of a connection element, a compressive force was developed in the link slab. No improvement in the response and load carrying capacity of the beams was observed due to debonding. Instead, there was a decrease in the ultimate load. For beams supported by hinges at each side of the connection, the behavior and stiffness of the debonded beams were comparable to that of a fully continuous beam under service load. For beams with different support conditions at each side of the connection element, the increase of their ultimate load and the overload responses were more significant for debonded beams under unsymmetrical loading. It was concluded that if the ultimate load criterion governed the design, then the optimum debonded length should be taken as 4% of the span length. However, if the deflection was the design criterion, the shorter debonded length corresponding to 2% of span length should be used. It was also indicated that similar stiffness was observed for all debonded beams within the service load range, irrespective of the loading type and support arrangement. The highest ultimate load was found for a debonding range of 2% to 6% of the span length, depending on the support conditions and loading. No significant difference

was observed in the responses of jointless decks with or without debond when subjected to temperature gradients. It is important to mention that the beams were supported by rollers and equally loaded.

2.2.1.3 Caner and Zia

Caner and Zia [1998] performed a series of tests on two jointless bridge decks to evaluate their behavior under static loading. The laboratory specimens consisted of a continuous reinforced concrete deck supported by either steel beams or prestressed concrete girders. The steel bridge was constructed with two 20.5 ft long simple-span steel beams (W12x26) that were placed with a 2 in gap between their two adjacent ends. The deck width and thickness were 24 in and 4 in, respectively. The concrete girders had 8 in width and 12 in height. Link slabs were detailed with a debonded zone equivalent to 5% of each adjacent bridge span to reduce stiffness and stresses (Fig. 2.1). This debonding was achieved by removing any structural mechanism capable of transferring load (e.g., stirrups and shear stud connectors) and by placing a bond breaker material between the beam and the deck. Link slabs were reinforced with three No. 6 epoxy coated bars.

Caner and Zia [1998] studied four different support configurations using pin and roller supports to observe differences in behavior of the jointless decks (HRRH, RHRH, RRRR, and RHHR). The authors concluded that the link slab behavior was independent of the support conditions since the measured reactions, strains, and deflections remained the same for all cases in the elastic range. The measured reactions and load-deflection curves of the girders indicated that each individual span behaved as if it was simply-supported. They observed that under service loading conditions (i.e., live load plus impact) the link slab cracked primarily due to bending. It was concluded that the main factors influencing the design of link slabs were bending and cracking. Fine flexural cracks were observed at the center of the link slabs. Caner and Zia [1998] justified this fact by arguing that issues associated with these cracks are less problematic than those resulting from leaking expansion joints. The authors recommended to use epoxy coated reinforcing bars to minimize the potential for reinforcement corrosion as well as a shallow transverse saw cut at the center of the link slabs. For horizontally restrained bridges, it was recommended the use of two layers of reinforcement to provide better crack control.

Caner and Zia [1998] found that previous analytical approaches developed by Gastal [1986] and El-Safty [1994] failed in predicting the behavior of the jointless decks. The discrepancy between test results and model predictions was attributed to the formulation of the link-slab element that was represented only with axial stiffness. Based on the findings of the study, the researchers provided methods for the analysis and design of link slabs. The analysis program

was used to determine stresses in the steel bars, and the surface crack widths at the mid-span of the link slab. All the bridge elements, including the link slabs, were modeled through conventional beam elements. The program was validated using the experimental results. The surface crack width was estimated by using the American Association of State Highway and Transportation Officials Specifications (AASHTO) code equation. The creep and shrinkage strains were determined using the tables given in PCI Design Handbook [PCI, 1992]. In the analysis, the moment of inertia of the cracked section was calculated and used for the center portion of the link slab if the moment in the link slab exceeded the cracking moment. Also, the reinforcement design for the link slab was revised until the criteria were met if the crack width exceeded 0.013 in.

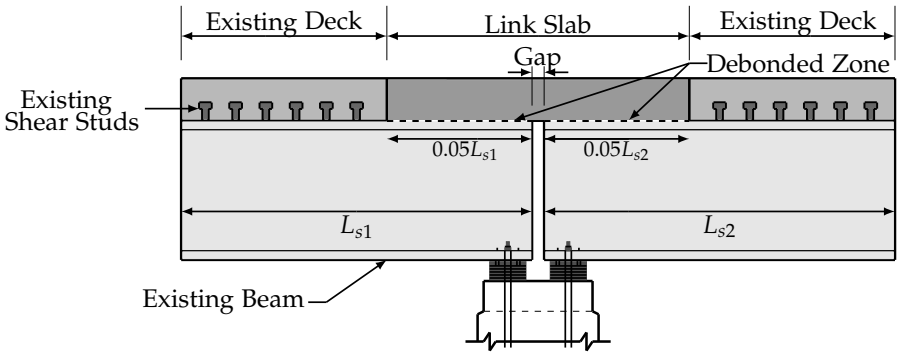

Figure 2.1: Debonded link slab configuration tested by Caner and Zia [1998]

Based on the laboratory study, Caner and Zia [1998] proposed the first formal design procedure for link slabs. This methodology is currently the most often used by DOTs in the United States. The procedure idealizes the link slabs as pin connections. It assumes that link slabs provide negligible continuity to the bridge system since they have lower stiffness compared to that of the girders. Therefore, the supporting bridge girders are considered to be fully composite with the deck and simply-supported for both dead and live loads. Further, link slabs are detailed with a debonded zone equivalent to 5% of each adjacent bridge span, as shown in Fig. 2.1. Link slabs are designed to resist the bending moments imposed by beam end rotations due to live load. The moment in the link slab (M_a) is calculated through Eq. 2.1 given by:

$$M_a = \frac{2E_c I_{ls}}{L_{ls}} \theta_g \tag{2.1}$$

where, E_c= elasticity modulus of the link-slab concrete; I_{ls}= moment of inertia calculated using the gross section properties of the link slab; L_{ls}= total length of the link slab; and θ_g=

maximum end rotations of the girders as simply-supported. The total length of the link slab L_{ls} is calculated as the sum of the debonded region at each adjacent span and the gap between them (Fig. 2.1).

The design criteria are the stress in the reinforcement and the maximum crack width at the tension face of the link slab. The amount of reinforcement in the link slab is obtained using a conservative reinforcing stress of 40% of the yield strength. The crack control criteria of the AASHTO specifications are applied to limit the crack width on the surface of the link slabs.

2.2.1.4 Wing and Kowalsky

Wing and Kowalsky [2005] conducted research to validate the design methodology and the limit-states, and to evaluate the long-term performance of link-slab jointless bridges. This study was the first demonstration of a link slab installed in North Carolina (Fig. 2.2). In the field program, a rehabilitated bridge structure was monitored over one year. The bridge structure initially had three interior expansion joints. After the bridge rehabilitation, only the center expansion joint was kept, and the other two were replaced with link slabs. The design procedure developed by Caner and Zia [1998] was used for the design of the link slabs with an established girder end rotation of 0.002 rad. The bridge was instrumented to measure temperature, strain, and deflections. After the bridge opened to traffic, the short-term monitoring for thermal and traffic loads was made. Live load tests were performed with four different load levels positioned at two selected locations. The first location intended to produce the maximum positive moment in one of the spans near to the link slab, whereas the second location, the maximum negative moment in the link slab. The applied loads were 31, 48, 68, and 95 kips. The performance limit states of link slabs were defined by residual crack widths and girder end rotations induced due to thermal or service loading. According to the authors, the range of temperature variations throughout a typical day could be more than 59 °F while the annual temperature variations could exceed 113 °F. Based on the investigation, it was found that the assumption of simply supported spans for dead and live load was acceptable although conservative. The thermal induced rotations were generally higher than those produced due to traffic loads. The crack size in the link slab exceeded the design criteria. The large crack (i.e., width of 0.063 in) was due to the saw cut which forced all the deformation into one crack. A larger limit for crack width was suggested to be investigated for link slabs having a saw cut. Several design charts were developed for different steel ratios based on the geometry of the bridge. In addition to the experimental studies, an analytical model of the entire bridge was developed to predict its performance under specified loads. The model was used to predict the girder end rotations during the live load test. The link slab was modeled as a pinned connection at the girder end bearings of the two adjacent girders.

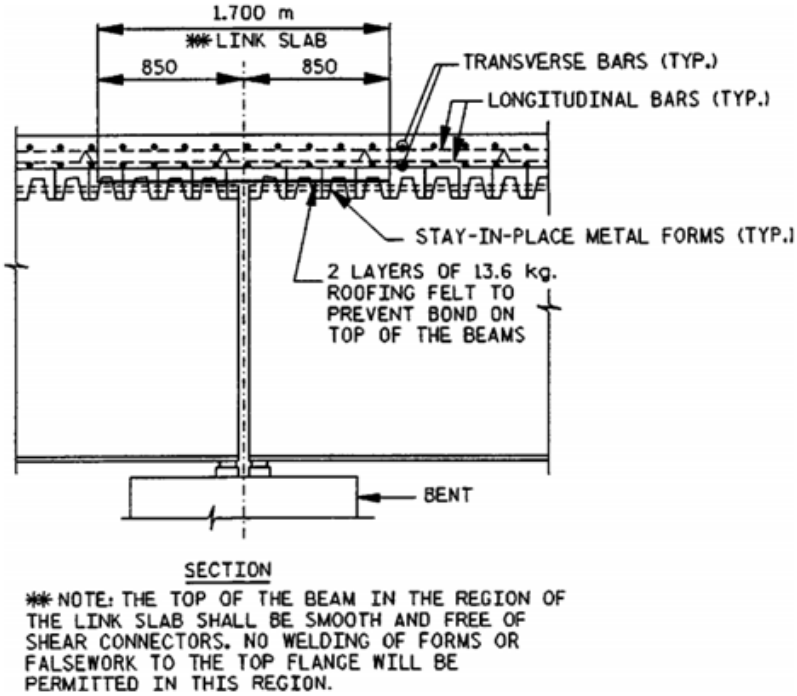

Figure 2.2: Link slab detail [Wing and Kowalsky, 2005]

2.2.1.5 Okeil and El-Safty

Okeil and El-Safty [2005] introduced the effects of the support conditions on the link slab system. The authors developed a simplified method for the flexural analysis of bridges with jointless decks that involves an extension of the classic three-moment equation. Okeil and El-Safty [2005] analyzed the link slabs as a partially continuous system since they prevent free rotation of the girders and the imposed rotations at their ends were not equal. As part of the investigation, several expressions for the tension force and the continuity moment at the link slabs were derived for two support arrangements, RHHR and HRRH. These configurations were selected because they corresponded to the upper and lower bounds of the behavior, respectively. In the derivation of the equations, it was assumed that link slabs only contribute axial stiffness ignoring any flexural rigidity they may provide. The proposed equations were validated using experimental data from Caner and Zia [1998]. From the comparison, Okeil and El-Safty [2005] reported discrepancy between the deflection test results and the theoretical results for the RHHR configuration. The authors explained that this difference was due to support movements that would prevent the development of large continuity moment [Okeil and El-Safty, 2005; El-Safty and Okeil, 2008]. A two-dimensional finite element model was

developed to check their hypothesis. The model consisted of a two-span bridge with a 7.5 in thick concrete deck. Plane elements were used to model the web of the steel beams and the reinforced concrete deck. Truss elements were used to model the flanges of the beams and the link slab. Okeil and El-Safty [2005] evaluated four configurations including simply-supported, HRRH, RHHR, and fully continuous. They found that the results from the finite element model were in good agreement with those of the proposed method.

Okeil and El-Safty [2005] performed a parametric study on a two-span link slab bridge to evaluate the effects of parameters such as girder types, support conditions, steel reinforcement ratios, and loading arrangements. The analytical results showed that the stiffness and tension force developed in the link slab were remarkably affected by the type of support configuration. Higher tensile forces in link slabs were observed when hinged supports were used. A debonded length between 2% and 6% of the girder span, depending on the support and loading conditions, was found to be adequate to obtain the maximum load capacity in the link slab. The increase of the steel reinforcement ratio in the link slab to an allowable limit (i.e., 6% and 3% with and without debonding, respectively) led the response of the bridge to be close to a continuous system. The authors recommended to further investigate the influences of skew, distribution of reactions and pier loads, and thermal and long-term effects.

2.2.1.6 Caner et al.

Caner et al. [2002] and Sevgili and Caner [2009] evaluated the seismic performance of bridges retrofitted with link slabs through analytical models. Caner et al. [2002] investigated the seismic response of link slabs over precast, prestressed concrete girders and varied superstructure support arragements. Based on the analytical work, seismic design guidelines were provided. Sevgili and Caner [2009] studied the seismic performance of skewed bridges in terms of forces and displacement when link slabs are used. The seismic response of various bridges with varied span lengths and skew angles was examined through elastic dynamic and nonlinear time history analyses. It was observed that link slabs can be implemented in bridges located in high seismic zones. A new reinforcement design for joint elimination at the abutments was developed.

2.2.2 Michigan Department of Transportation (MDOT)

2.2.2.1 Li et al.

Li et al. [2003] proposed the detail show in Fig. 2.3 to address the interfacial cracking problem of conventional link slabs, caused by high-stress concentrations at the interface between the link slab and the existing concrete deck. As seen in Fig. 2.3, the proposed detail had a transition zone of 2.5% at each adjacent span in addition to the debonded zone of 5%. This

transition zone served to move the interface away from the start point of the debonding. Notice that there were shear studs in the transition zone, so composite action between girder and link slab was developed in this region. In addition to the modified design detail, Li et al. [2003] introduced the use of engineering cementitious composite (ECC) for link slabs. ECC is a concrete material with high ultimate tensile strain capacity (up to 4%) that allows microcracking [Lepech and Li, 2008, 2009]. The proposed design detail was tested under monotonic and cyclic loadings.

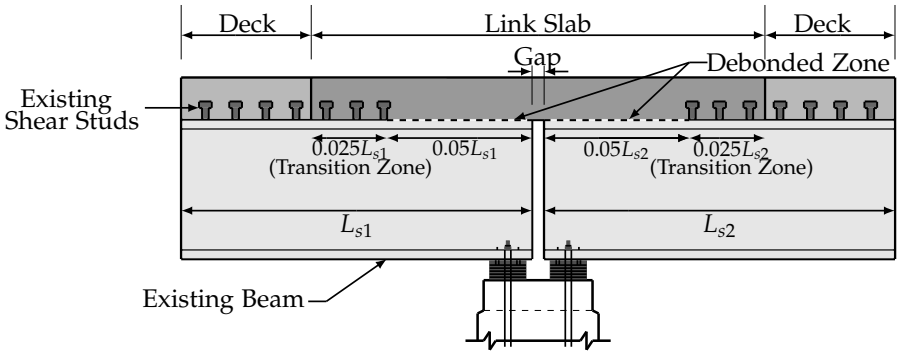

Figure 2.3: ECC link slab configuration proposed by Li et al. [2003]

Li et al. [2003] reported design guidelines for ECC link slabs (Fig. 2.3). In the guidelines, the total length of the ECC link slab (L_{ls}) was calculated through Eq. 2.5 in terms of the span lengths (L_{s1} and L_{s2}) and the spacing between the adjacent spans (Gap):

$$L_{ls} = 0.075\,(L_{s1} + L_{s2}) + Gap \tag{2.2}$$

The length of the debonded zone L_{dz} was calculated as:

$$L_{dz} = 0.05\,(L_{s1} + L_{s2}) + Gap \tag{2.3}$$

The maximum end rotation angles of the adjacent bridge span due to live load was determined as a function of the maximum allowable deflection and the length of the adjacent spans, as shown in Eq. 2.4.

$$\theta_{max} = \Delta_{max}\left(\frac{3}{L_s}\right) \tag{2.4}$$

where θ_{max} is the maximum end rotation angle of the adjacent bridge spans in radians and Δ_{max} is the maximum allowable deflection of the shorter of the two spans in mm.

Li et al. [2003] found that the stress in the reinforcement is not a suitable criterion to determine the required reinforcement ratio in the link slabs. The authors stated that the use of an uncracked section for the calculation of the applied moment value in the link slabs leads to an overestimation of the required amount of longitudinal reinforcement to satisfy the limit stress criterion. Therefore, the design method by Li et al. [2003] calculates the amount of steel reinforcement in the link slab based on the moment capacity of the section. A non-linear sectional analysis is used for the calculation of the moment capacity assuming that ECC material remains perfectly elastic-plastic in service. Conservative working stress of 40% of the yield strength of the steel reinforcement was used for design.

In a later study, Li et al. [2005] performed the field demonstration of the improved design detail shown in Fig. 2.3 in a bridge in Michigan. Cracking was observed three days after placement and before curing was completed. Several cracks developed within the link slab. The cracks were 0.005 in. to 0.014 in wide and spaced approximately 8 in. They tended to originate from the steel bars and propagate radially outward. The most severe cracking was observed around the rebar which protrude out of the link slab surface to be cast into the sidewalk. The cracking was attributed to temperature gradients, shrinkage stresses, or too much water loss at early ages.

Li et al. [2008] concluded that causes of the early age cracking could be low water-to-cement ratio, low-retarder-to-cement ratio, use of gravity-based mixer, high curing temperature, low curing relative humidity, wind effect, rebar as stress concentrator, and skew angle. It was recommended limiting the angle of skew angle to 25°, nightime casting, and water curing for at least 7 days.

2.2.2.2 Aktan et al.

Aktan et al. [2008] performed a field inspection of eight bridges in Michigan to determine the performance of link slabs and other bridge components such as approach slabs, sleeper slabs, backwalls and bearings. All the inspected link slabs were designed based on the procedure described by Caner and Zia [1998]. The design detail of the link slab is shown in Fig. 2.4 Notice from the detail that the bottom layer of the reinforcement was discontinuous. The main problems reported in the survey indicated the existence of full-depth transverse cracks of significant width at the centerline on the typical link slabs. The cracking was attributed to poor construction practices including insufficient placement of the longitudinal steel, lack of a pour sequence, and untimely saw cut.

Aktan et al. [2008] performed a 3D finite element model analysis to investigate factors affecting jointless bridge deck cracking. The model represented an existing bridge, and it

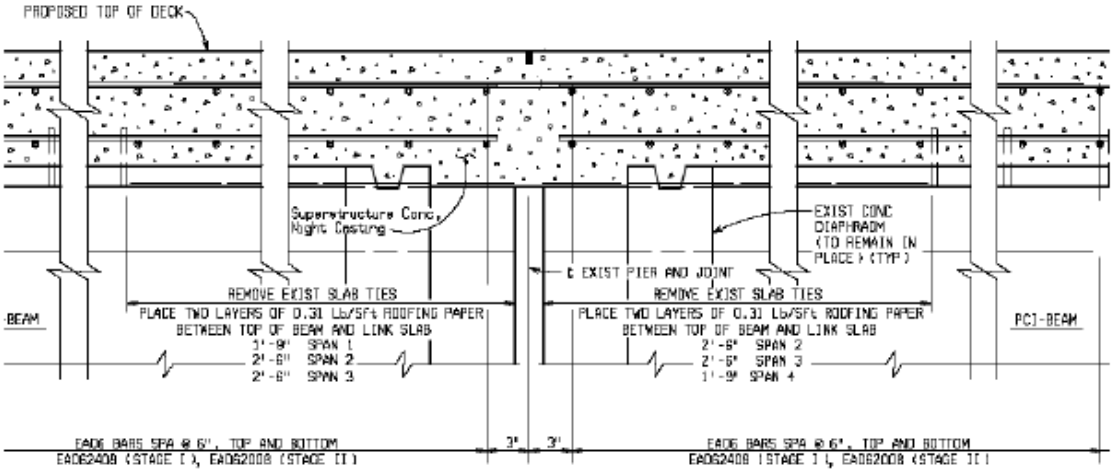

Figure 2.4: Link slab detail used in Michigan [Aktan et al., 2008]

consisted of a single girder, two 834 in spans, and 9 in thick concrete deck. The compressive strength for girder and deck was 5000 psi. Link slabs were modeled with the bottom reinforcement discontinued over the pier centerline. The design parameters investigated were support conditions, debonded length, girder height, and adjacent span length ratios. Three different support conditions were examined: HRRR, RHHR, and RRHR. Debonded length was varied as 0%, 2.5%, 5.0%, and 7.5% of the span length. The two standard PCI sections examined were Type III and Type VI. The effect of having unequal span lengths was investigated by increasing the second span from 69.5 ft to 91 ft. The total length of the link slab was also increased from 85 in to 98 in. The models were subjected to both live HL-93 and thermal loads for Zone 3, as specified by AASHTO [2017]. Straight and 20° skew two-span multi girder full-width models were developed for investigating load demand on link slabs and addressing additional issues from link slab torsion and twist that arise due to symmetric loading of single- and two-lane bridges.

Based on the analysis results, it was concluded that cracks on the link slabs were caused by thermal hydration and drying shrinkage stresses. It was observed that support conditions greatly influenced the behavior of link slabs. The link slabs were subjected to combined axial force and moment with RHHR support configuration. The analysis also showed that drying and thermal hydration shrinkage strains can generate cracks of which the width matched the expected magnitude under a live load. The authors recommended to include the additional moment and axial force resulted from thermal gradient loads into the link slab design. A new method for the analysis of link slabs was proposed that involved the use of an axial load versus moment interaction diagram for those specific support configurations in which the link

slabs were subjected to combined flexural and axial loads. Full-bridge link slab assemblage models revealed that torsional moment increased in link slabs of skew bridges irrespective of support conditions. The study recommended controlling cracking through the development of new cementitious materials. It was also suggested the use of continuous top and bottom reinforcements irrespective of support conditions as well as a saw cuts directly over the pier centerline and at each side of link slab to control cracking [Ulku et al., 2009].

2.2.2.3 Aktan and Attanayake

Aktan et al. [2008] proposed a design method based on the analysis of two-span bridge models with zero skew angle and subjected to live and thermal loads. Aktan and Attanayake [2011] then modified the procedure to incorporate the effects of the angle of skew on the link-slab moments. The investigation included finite element modeling of skew link slabs subjected to static truck-load and thermal gradients as well as field assessment of a skewed bridge. The influence of different bearing configurations on the link slab moment and force resultants was also examined. Design recommendations were developed for the utilization of link slabs in high skew bridges. The study determined that moment generated in a link slab under temperature gradient loads remained constant irrespective of the span. It was observed that the moment developed in a link slab under live load decreased with increased span. The researchers found the minimum reinforcement amount required by AASHTO specifications to be adequate for skew link slabs at specific support configurations (i.e., HRRR or RRHR). Additional reinforcement at the bottom layer was suggested to resist large tensile stresses that develop near the boundaries of the debonded region. It was also recommended a construction joint at the limit of debonded and fully bonded zones. Bridge deflections and bearing translations were measured under static truck as well as thermal loads.

2.2.3 Virginia Department of Transportation (VDOT)

2.2.3.1 Ozyildirim et al.

Ozyildirim et al. [2017] evaluated the performance of different types of concrete materials at eight rehabilitated joints using link slabs. Two of the link slabs were constructed using rapid-set cement and latex modified concrete (LMC). The other six link slabs were built using low-permeability fiber reinforced concrete (FRC) with various class of fibers. The three types of fibers used were polivynil alcohol, polypropylene, and steel. All concrete mixtures were designed to have a compressive strength of 3000 psi after 24 hours. Bridge surveys were conducted to assess the performance of the materials, based on the observed cracking. A maximum permissible crack with of 0.004 in. was established for resisting water penetration. The study reported low shrinkage and wider cracks using rapid-set cement with LMC. The

crack widths ranged from 0.004 in. to 0.016 in. All FRC mixtures showed high shrinkage and cracks widths less than 0.004 in. Further research was recommended to reduce shrinkage in the FRC mixtures with polypropylene or steel fibers due to their satisfactory performance.

2.2.3.2 Hoomes et al.

Hoomes et al. [2017] evaluated the mechanical properties and performance of high-performance fiber reinforced concrete (HPFRC). The different HPFRC mixtures investigated were: ECC, hybrid fiber-reinforced concrete (HyFRC) with steel and synthetic fibers, HyFRC with only synthetic fibers, and UHPC with steel fibers. Different tests were carried out in the fresh concrete such as air content, density, slump cone, mini-slump flow, and inverted slump cone. Tests on hardened concrete tests were conducted to determine compressive, flexural, and bond strengths. Shrinkage was also evaluated in different mixtures. According to the authors, ECC and UHPC mixes were self-consolidating and workable. HyFRC mixtures were workable but required consolidation. Fibers in ECC and HyFRC were well disbursed, but not for the UHPC samples. It was observed that for the UHPC mix, the fibers settled at the bottom. All concrete mixes, except UHPC, showed deflection hardening. This fact was attributed to the settlement of the fibers. The authors concluded that HyFRC with synthetic fibers provided the most economical solution for crack control and bond strength. A further field application using this material was recommended.

2.2.4 New York State Department of Transportation (NYSDOT)

2.2.4.1 Royce

Royce [2016] presented several case studies in his paper on the utilization of ultra-high performance concrete (UHPC) in the State of New York. He provided the history of the development of the field-cast UHPC among precast elements along with the lessons learned in each of these case studies with little emphasis on the link slabs. He stated some of the most important factors for the success of these joints. He mentioned that tight leak-free formworks were essential during the construction to ensure the strength of these joints. Moreover, careful storage of the premix powder was needed to prevent moisture from creating silica balls of the powder resulting in inefficient mix. In addition, the application of heat for several hours in the curing of the joint would result in a desirable speed in strength gain. He noted that the utilization of the UHPC was advantageous in terms of the gained speed of construction.

The author dedicated a small section about the use of the UHPC in link slab construction in New York. He claimed that UHPC was able to accommodate girder end rotations as the UHPC could develop ultimate tensile strains up to 0.0007. The NYSDOT link slabs designs have been effective as no visible cracks were reported on the link slabs constructed. However,

he stated that proper design was crucial as there were several factors affecting the performance of the link slab. He noted, also, that a faulty link slab design, might not only result in cracks on the link slab but also structural deterioration of other bridge components.

Fig. 2.5 shows an example of a design detail implemented by NYSDOT. It corresponds to a partial-depth cast-in-place link slab. This connection detail was implemented to rehabilitate the SR962G bridge over US Route 17 in Owego, New York. The bridge rehabilitation project involved the use of precast concrete deck panels. The filler material used in the connection was UHPC [Graybeal, 2014].

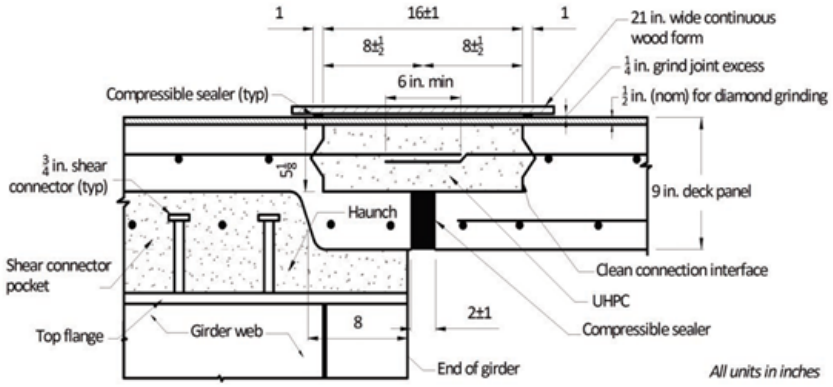

Figure 2.5: UHPC link slab detail [Graybeal, 2014]

2.2.5 Hawaii Department of Transportation (HDOT)

2.2.5.1 Reyes and Robertson

Reyes and Robertson [2011] introduced precast link slab details using high performance fiber reinforced cementitious composite (HPFRCC) reinforced with glass fiber reinforced polymer (GFRP). The proposed link slab was a thin slab of thickness less than the deck slab. The study utilized full scale experimental test of three specimens of full scale expansion joints that included part of the adjacent steel girders, as shown in Fig. 2.6. The girders in the test were loaded statically for cycles of loads to simulate the traffic load and ensure the elastic response of the detail. The first specimen tested was a cast-in-place link slab. Although this specimen showed better continuity at the connection between the link slab and the deck compared to the other two specimens, it showed lower compressive strength capacity. The other two specimens were pre-cracked precast link slabs connected to the deck slab via anchors/dowels. The authors argued that the precast slabs were advantageous as precracking was possible giving the link slab more ductility and increasing the effectiveness of the slab in compression. A

drawback in the precast link slab that needed more research was the weak continuity between the slab deck and the link slab. The outcome of this study was that precast link slab was a viable solution for quick retrofitting of the bridges.

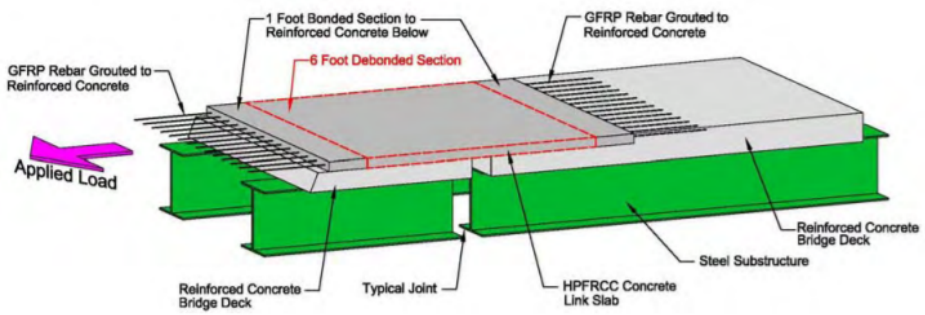

Figure 2.6: HPFRCC precast link slab tested by Reyes and Robertson [2011]

2.2.5.2 Larusson et al.

Larusson et al. [2013] developed a link slab detail using ECC and GFRP reinforcement. The new link slab design featured a relatively thin, prefabricated link slab element composed of highly ductile ECC and reinforced with low stiffness GFRP reinforcement. The design detail tested by Larusson et al. [2013] is illustrated in Fig. 2.7. An experimental program was carried out on four link slabs to assess the proposed design. The experimental investigation focused on the load deformation response and crack development of flexible elements during both monotonic and cyclic action. The two-span bridge specimens represented a link slab installed on steel girders. Cast-in-place and prefabricated link slabs were used. The authors concluded that the design concept showed promising results according to load response and crack development. Additionally, the use of GFRP improved corrosion resistance due to its noncorrosive nature. Although the prefabricated link slab investigated in this study was designed to enable both unrestrained rotation as well as axial length changes, the experimental program carried out focused solely on axial deformations.

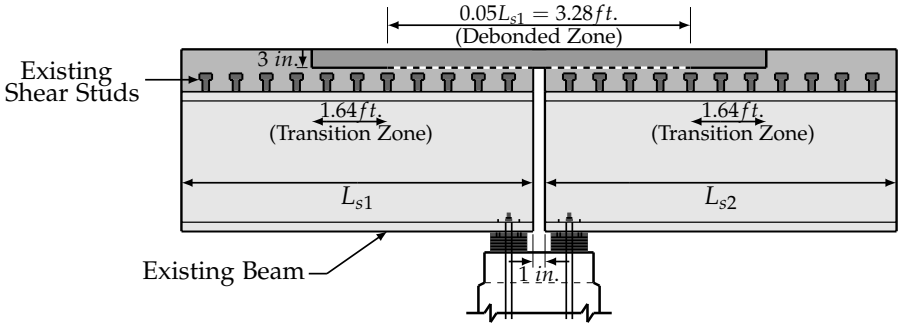

Figure 2.7: GFRP link slab detail

2.2.6 Louisiana Department of Transportation (LaDOTD)

2.2.6.1 Li and Saber

Li and Saber [2009] investigated experimentally and numerically the use of corrosion resistant FRP grid reinforcement in developing durable ductile link slabs in jointless bridges. The experimental program presented by them included material testing to identify the various material properties such as modulus of elasticity, Poisson's ratio, and coefficient of thermal expansion, specimen testing via 3-point flexure test on FRP reinforced slabs to evaluate the composite behavior in bending, and full-scale beam testing to evaluate link slab performance under dead and live loads. The tested link slab detail was a debonded link slab with added two FRP grid reinforcements 1 in apart of 1 in thickness slightly below the mid of the section as shown in Fig. 2.8.

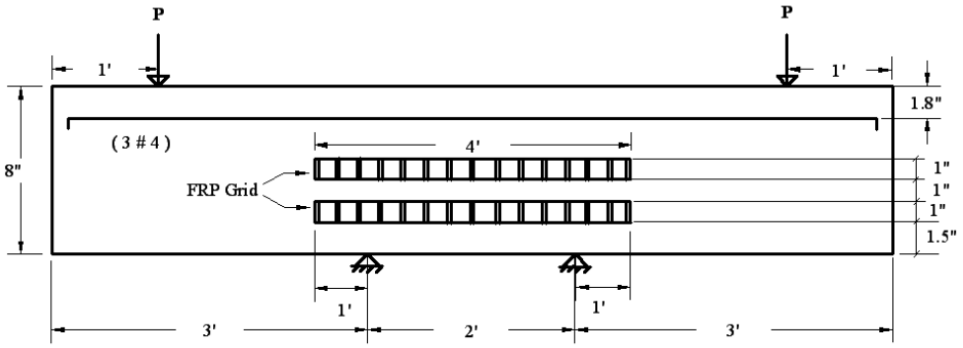

Figure 2.8: Full-scale beam testing setup as presented by Li and Saber [2009]

The numerical analysis presented in the study is a finite element analysis on a three-span bridge under dead and live loads. The link slab modeled in the analysis was a FRP grid reinforced debonded link slab. The study showed that although the lab-manufactured FRP had higher ultimate strength, the commercial FRP exhibited more deflection, which was favorable for link slabs. The study, also, concluded from both analyses that the commercial FRP reinforced link slab significantly reduced the stresses in both the girders and the slabs as it provided high ductility to the slab. The proposed slab showed advantageous reduction in the shrinkage and the thermal coefficients compared to the conventional reinforcement.

2.2.7 Ministry of Transportation of Ontario (MTO)

Ontario is one of the provinces of Canada that most implement link slabs in their bridges. Research conducted by Lam et al. [2008] and Lam [2011] documented different design details used by the Ministry of Transportation of Ontario (MTO). Lam [2011] reported three different link-slab configurations: haunched, flexible, and debonded. The haunched and flexible configurations were used for deck rehabilitation during the early 1990s. Lam [2011] indicated that it has been discontinued the use of these details because of their high costs as well as limitations in the girder end-rotations and girder depth. Both details are shown in Fig. 2.9 and their full description can be found in Lam et al. [2008]; Lam [2011].

Au et al. [2013] introduced an adjustment factor for the link-slab moment equation (Eq. 2.1). According to the researchers, Eq. 2.1 did not account for the compatibility of displacement between the link slabs and the supporting girders properly. Au et al. [2013] observed unrealistic deformation patterns when three-dimensional analyses were conducted. The revised moment demand by Au et al. [2013] is given by Eq. 2.5:

$$M_a = \frac{2E_c I_{ls}}{L_{ls}} \theta_g \alpha_R \tag{2.5}$$

The adjustment factor α_R in Eq. 2.5 is given as a function of the distance between adjacent simple supports at the pier location (Gap), as follows:

$$\alpha_R = \frac{4}{\left(1 + \frac{3Gap}{L_{ls}}\right)} \tag{2.6}$$

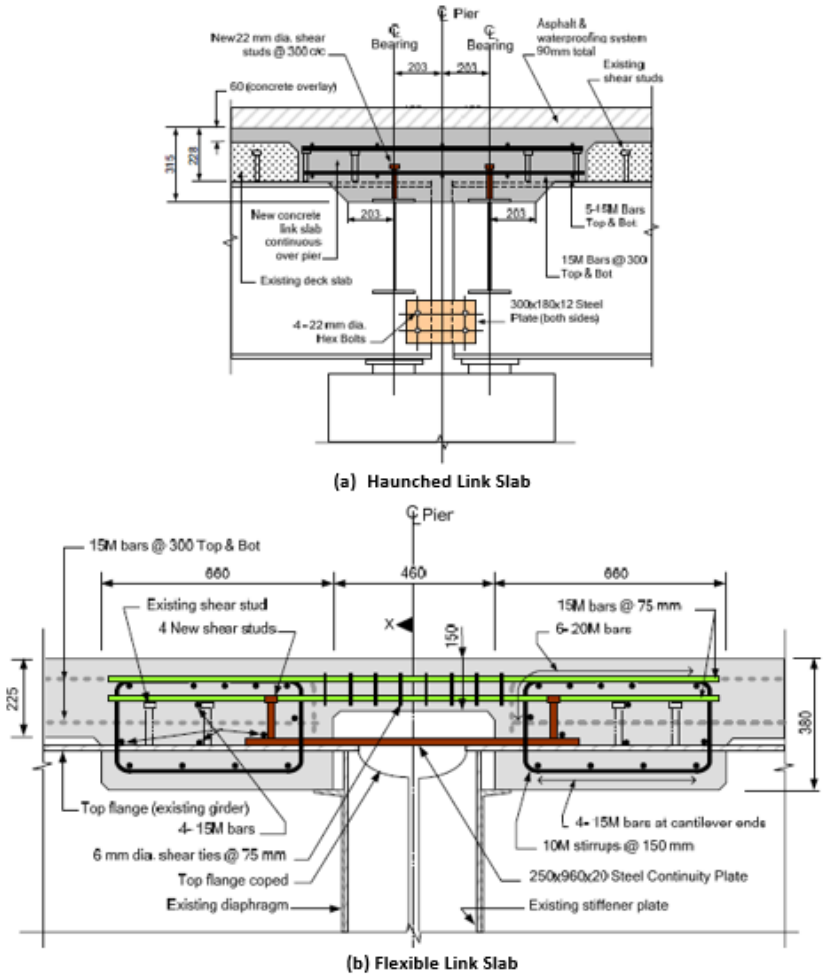

Figure 2.9: Link slab details used in Canada [Lam et al., 2008]

2.3 Design Specifications and State Construction Practices

The AASHTO Standard Specifications [AASHTO, 2017] do not provide guidelines for the design and detailing of link slabs. In a recent study by Culmo et al. [2017], the researchers provided general design provisions for accelerated bridge construction (ABC) for incorporation into future bridge specifications. The review of current standard specifications, as well as the proposed ABC AASHTO guidelines, shows that the majority of DOTs follow the approach concept proposed by Caner and Zia [1998] described in Section 2.2.1.3 to design the link slabs. Link-slab design details and practices vary depending on the transportation agency. Not all the agencies that have implemented link slabs in their bridges provide guidelines. The spe-

cific standard provisions available for the design of link slabs, design details, and practices in the states of North Carolina, Virginia, New York, Massachusetts, Florida, and Utah are summarized below.

2.3.0.1 North Carolina

Section 8.2 of North Carolina Structures Management Unit Manual [NCDOT, 2018] recommends the use of link slabs for deck joint elimination on simple span superstructures. Section 6.2.2.4 of the same design manual states that link slabs shall be used for replacing the expansion joints over piers in bridges with span lengths not exceeding 75 ft. Both prestressed concrete girders (AASHTO Type II and III) and steel beams are the type of cross sections required by the specifications.

Current practice in North Carolina includes the use of full-depth link slabs with saw cuts at the center of the link slab. These saw cuts of 1.5 in deep are usually filled with a joint sealer material that is a low modulus silicone sealant. In addition, it is recommended the use of Class AA Concrete (4500 psi), two layers of epoxy continuous steel longitudinal reinforcement within the link slab, and transverse construction joints located at the limits of the link slab (Fig. 2.2). No welding of forms of falsework to the top of girder are permitted in the link slab area.

2.3.0.2 Virginia

Section 412.03 of the Virginia Standard Specifications [VDOT, 2016a] addresses the repairing process of bridge decks at piers using link slabs. It states, "*Deck Slab Closure shall consist of repairing bridge decks for link slabs at piers and deck extensions at abutments in accordance with the plan details and the requirements herein. This work shall consist of removing and disposing of existing concrete and any existing joint armor, removing and disposing of stud shear connectors within the limits of the slab closure for steel beams/girders, removing and disposing of stirrup bars within the limits of the slab closure for concrete beams/girders, repairing or replacing existing reinforcing steel as may be required by the work described in this Section, preparing the contact surfaces, furnishing and placing expanded polystyrene, and furnishing and placing new reinforcing steel and concrete in accordance with the details and requirements herein. Exposed undamaged existing reinforcing steel shall be abrasive blast cleaned and reused. The contractor shall develop a sequence of construction for deck slab closures to be used in conjunction with other related work items (bearing modifications, etc.) which shall be submitted to the Engineer for review prior to performing the work. The cost of preparing the sequence of construction shall be included in the price for deck slab closure*."

The Virginia Manual for Bridge Element Inspection [VDOT, 2016b] states the different defects that shall be inspected in the link slabs, such as concrete delamination, spalls, patched

area, exposed rebar, efflorescence, rust staining, cracking, abrasion, leakage, and severe damage caused by impact. The manual establishes a link slab in good condition if none of the previous defects are observed and if the cracks are less than 0.012 in in width or spacing more than 36 in. No abrasion or wearing is permitted. Link slabs are defined as element 843 in the manual that defines joint closures constructed at piers. Slab extension is the element 844 that defines joint closures constructed at abutments.

Section 32.09 of the Manual of the Structure and Bridge Division [VDOT, 2018] addresses the guidelines for bridge deck joint elimination. The manual states that link slabs should be used together with concrete overlays to provide additional protection over the cold joint between the existing deck and the link slab or deck extension. The overlays should be placed after the completion of the link slabs. For projects involving hydromilling, the placement of the link slabs before to hydromilling is recommended for convenience in handling the water produced during the process. The manual establishes a state goal of eliminating 2% of the expansion joints in each District per fiscal year.

The VDOT bridge manual specifies the use of flexible link slabs on existing bridges in which the existing deck is not replaced or on new decks where the superstructure is not replaced. It is also recommended, once the link slabs are installed, the structural design checking of existing bridge elements as bearings, piers, and remaining joints. The bridge manual states that jointless bridges with link slabs and spans less than 120 ft do not require analysis if meet the following requirements:

1. *Compressive strength of concrete in link slab is equal or greater than 4000 psi.*
2. *Longitudinal reinforcing steel from existing concrete deck is spliced to reinforcement in link slab through lap splice or mechanical coupler; spacing not to exceed 12 in.*
3. *Transverse reinforcing steel is replaced and spliced, if necessary for staged construction.*
4. *Link slab length is 2 ft in either direction from the center-line.*
5. *Shear connectors are removed and a bond braking material is placed within the area of the link slab*

The Virginia standard detail for the link slabs is shown in Fig. 2.10. This detail is allowed to be used for a maximum bridge span length of 100 ft. In addition, it is required that both of the adjacent bearings supporting the beams at the joint allow horizontal movement. The use of elastomeric expansion bearings is encouraged as they help transfer longitudinal forces to the substructure and minimize the redistribution of loads due to changing fixed/expansion bearing relationships. Concrete materials for the construction of link slabs must be Low Shrinkage Class A4 Modified Concrete 4000 psi.

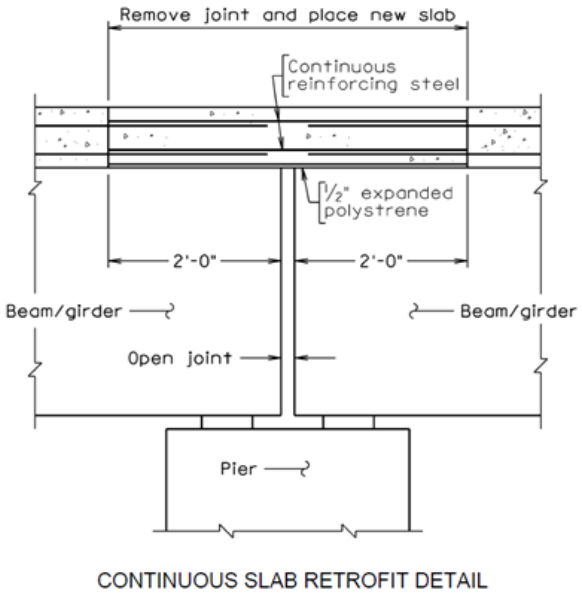

Figure 2.10: VDOT link slab detail [VDOT, 2018]

2.3.0.3 New York

The New York State Bridge Manual [NYSDOT, 2018] defines the link Slabs as:

"*A concrete link slab is a relatively thin reinforced concrete slab or UHPC slab that typically connects simply supported deck spans. It is designed to flex due to girder deflections and transmit compressive and tensile forces through the deck in conjunction with appropriately designed bearings.*"

Article 19.7.1 of the New York state Bridge Manual addresses the general design considerations for joint elimination. For projects with full deck replacement, conventional link slab (CIP decks) or UHPC link slab (precast decks) is the priority for joint removal at intermediate supports. For projects with deck retention, it is recommended only to use UHPC link-slabs. The UHPC link-slab detail is shown in Fig. 2.11. Section 5.2 of the manual addresses the jointless deck analysis and design. Article 5.2.3 specifically discusses jointless decks at piers. Article 12.2.8 says that the design and detailing of bearings for bridges with link slabs is complex and shall be accomplished together with the Office of Structures of the state.

The NYSDOT [2018] bridge manual requires a bond breaker along the top flange at the ends of the girders near the pier to allow the slab to flex independently of the girder, reducing the negative bending moment in the slab. A contraction joint shall be provided in any concrete

pour over the link slab location (barrier, sidewalk, curb, etc.). Link slabs are designed to flex with girder deflections as well as to transmit compressive and tensile loads between the spans. The design is influenced by, but not limited to, span arrangement, bearing type and arrangement, girder end rotation due to live load, bridge skew, and girder depth.

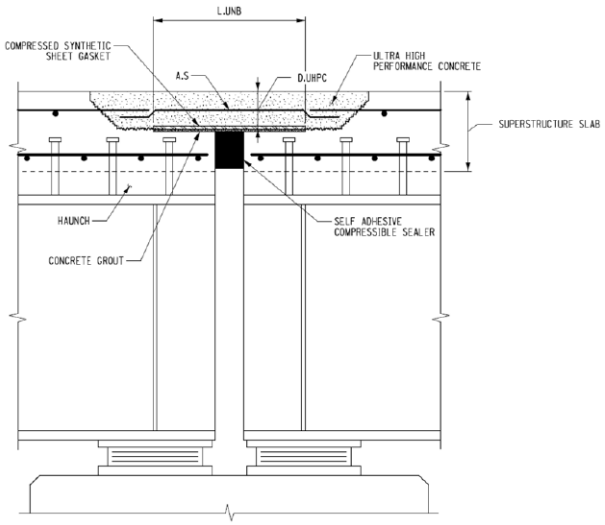

Figure 2.11: NYSDOT link slab detail [NYSDOT, 2018]

2.3.0.4 Massachusetts

Article 3.5.2.5 of the Massachusetts LRFD Bridge Manual [MassDOT, 2013] addresses the link slab design provisions. A general procedure for the design of link slabs can be summarized as follows:

1. *Design adjacent spans as simply supported neglecting the proposed link slab.*
2. *Determine the length of the link slab using approximately 5% to 7% of each span length. The link slab requires debonding from the girder and thus no shear stud connectors shall be provided.*
3. *Determine the end rotations of the girders from the beam design under service (unfactored) live loads. If the software used does not provide end rotations, the end rotations can be determined using the midspan deflections. The end rotation may be estimated as equal to* $3.2\Delta_{LL}/L$.
4. *Calculate the negative moment in the link slab due to service load rotations,* M_a*, using the gross section properties of the link slab. Calculate cracking moment of link slab,* M_{cr} *[Article 5.7.3.6.2-2 AASHTO [2017]]. If* $M_a > M_{cr}$*, then cracks can be expected in the link slab and additional reinforcement is required.*

5. *Design the reinforcement for the link slab to resist the applied moment using working stress methods and check the control of cracking criteria per Article 5.7.3.4 AASHTO [2017]. Use γ_e, of 0.75 for Class 2 exposure condition. The tensile stress in the reinforcement, f_{ss}, shall not exceed $0.4f_y$.*

2.3.0.5 Florida

Section 8.7 of Florida Structures Design and Detailing Manual [FDOT, 2018] addresses the provisions for elimination of deck expansion joints. Article 8.7.2 states the provisions for continuous deck over simple span piers (i.e., link slabs). The debonded zone at each span is determined as $L_s/20$, where L_s is the span length. Moment demand in the link slabs is calculated following the design methodology proposed by Caner and Zia [1998] for bridges with span-length less than 100 ft. Detailed analysis is required for computing girder end rotations in longer bridges.

2.3.0.6 Utah

Article 21.5.2.5 of Utah Structures Design and Detailing Manual UDOT [2017] states the following about the use of link slabs:

"*Use link slabs to eliminate joints between simple spans where integral diaphragms are not feasible. A link slab is constructed by removing the joint and several feet of deck on each side of the joint, and replacing the joint with a concrete slab that is not bonded to the girder. The treatment can eliminate the leaking joint and minimize repair costs and impacts.*"

Table 2.2 summarizes the above mentioned information regarding state practices.

Table 2.2: Summary of state practices

Practice	State					
	North Carolina	**Virginia**	**New York**	**Massachussets**	**Florida**	**Utah**
Max. span length	75 ft	100 ft	NA	NA	100 ft	NA
Beam cross section	AASHTO Type II and III and steel girders	PC and steel girders	NA	NA	NA	NA
Max. skew angle	NA	NA	30	NA	NA	NA
Concrete type	Class AA Concrete (4.5ksi)	Low Shrinkage Class A4 Modified Concrete (4 ksi)	UHPC (21 ksi)	NA	NA	NA
Link slab configuration	Full-depth	Full-depth	Partial-depth	Full-depth	Full-depth	Full-depth
Debonded length	5% of each span	2 ft of each span	2-3 ft of each span	5-7% of each span	Ls/20	NA
Bearing types	Elastomeric bearings	One bearing must allow horizontal movement	Do not use two lines of fixed bearings Do not use with steel rocker or steel sliding bearings	NA	NA	NA
Design criteria	Live load girder end rotations and AASHTO crack width criteria					
Curing	wet curing 7 days					

Note: NA = Not Available.

2.4 Assessment of Existing Indiana Link Slab Bridges

The aim of this section is to assess the performance of the existing Indiana bridges that include link slabs based on field observations. A list of these bridges is obtained from the INDOT personnel that is then refined by validating the existence of link slabs in each of these bridges. Fig. 2.12 shows the location of the bridges. The assessment is based on the inspection reports and drawings obtained via the INDOT BIAS system. The assessment includes the identification of the detail used in the bridge as well as the reported bridge conditions in the various inspection reports over the years preceding and following the link slab installment. Tables 2.3 and 2.4 present the geometric properties of the bridges as well as the link slab attributes, respectively. It is important to note that the inspection reports are general subjective visual inspections of the whole bridge (not specifically for the link slabs) with no quantitative evaluations of the cracks (i.e., number of cracks, crack depth, exact locations, etc.). The bridge condition assessment is based on what is reported in writing by the inspectors on the superstructure. The assessment for each of the identified bridges is presented below.

Figure 2.12: Location of the existing link slab bridges

Table 2.3: Summary of geometric properties of Indiana link slab bridges

Bridge	Year Built	Girder Type	Structure Type	Number of Spans	Max. Span Length [ft]	Total Length [ft]
Captain Frank	1965	Prestressed Concrete	Multi-beam	3	50	120
SR64/SR37	1956	Concrete	Multi-beam	5	41	181
Owensville	1966	Concrete/Steel	Continuous Steel/Multi-beam Concrete	4	60	200
SR68/I64	1966	Concrete/Steel	Continuous Steel/Multi-beam Concrete	4	68	223
Hillcrest/US50	1961	Concrete/Steel	Continuous Steel/Multi-beam Concrete	5	80	277
I90/CR900	1956	Steel	Multi-beam	3	34	117
I90/Tamarack	1956	Steel	Multi-beam	3	35	113

Table 2.4: Summary of inspection reports of Indiana link slab bridges

Bridge	Link Slab Rehabilitation	Link Slab Type	Inspection Date	Crack Location
Captain Frank	1992	Haunched	2000-2017	Girders at supports
SR64/SR37	2016	Haunched	2006-2016	Link slab
Owensville	2015	Haunched	2008-2018	Typ. girder flexural
SR68/I64	2015	Haunched	2007-2018	Increased underside deck cracking and spalling adjacent to upper flange
Hillcrest/US50	2017	Debonded	2007-2017	No cracking reported
I90/CR900	2013	Not Identified	2007-2017	Heavy map cracking of deck, deck spalling, significant leakage at link slab
I90/Tamarack	2013	Not Identified	2007-2017	Link slab

2.4.1 I-64 EB/WB over Captain Frank Road

The rehabilitation plans for this bridge dates back to 1992. The plans show the removal of all intermediate expansion joints and the installment of link slabs. A design detail of the link slabs is shown in Fig. 2.13. It can be observed that the link slab is a haunch type detail with no debonding provided.

No inspection has been reported before the link slab construction. Nine inspection reports between 2000 to 2017 are available for this bridge. According to these reports, the bridge is exhibiting cracks and showing deterioration in both the deck and the supporting girders. It is clear that there is consistent deterioration near the abutments as more than 10 beams are experiencing this type of deterioration. However, due to the lack of inspection reports before

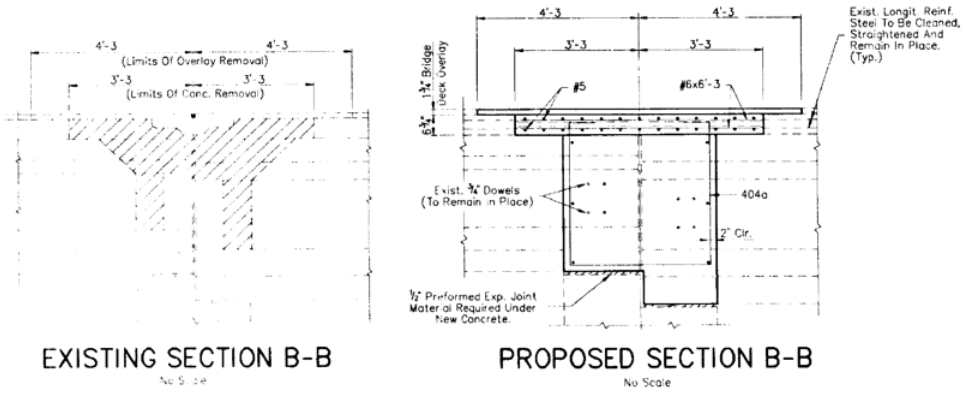

Figure 2.13: Link slab detail (I-64 over Captain Frank)

the link slab installment or even reports in the early years following the installment, it is difficult to attribute the deterioration to the link slab installment.

The last visual inspection to this bridge was conducted on November 6, 2017. Both eastbound and westbound were inspected. It was reported fair condition for both the superstructure and the wearing surface. Satisfactory condition with minor deterioration was reported for the deck and substructure. The inspector did not provide any specific information about the condition of the link slab.

2.4.2 SR 64 over SR 37

According to the inspection report, the bridge rehabilitation was performed in 2016. All expansion joints over intermediate piers were eliminated using link slabs. A design detail of the link slabs is shown in Fig. 2.14. It can be seen from the figure that a 1 in haunch was used at the end of the girders. In addition, an overlay of latex modified concrete (LMC) was provided on top of the slab. A gap of 1 in between the girders was used in all bents except in those located between the middle spans. A debonded zone for this particular link slab was not provided.

A total of six inspection reports are evaluated between the years 2006 till 2016. Five inspection reports have been reported before the link slab construction, while only one exists after the link slab construction just few months later. According to these reports the bridge exhibited slow deteriorations, mostly described as typical, over the years preceding the installment of the link slab. However, just few months after the rehabilitation cracks, though minor, started to occur in both the deck and the girders especially around the link slabs.

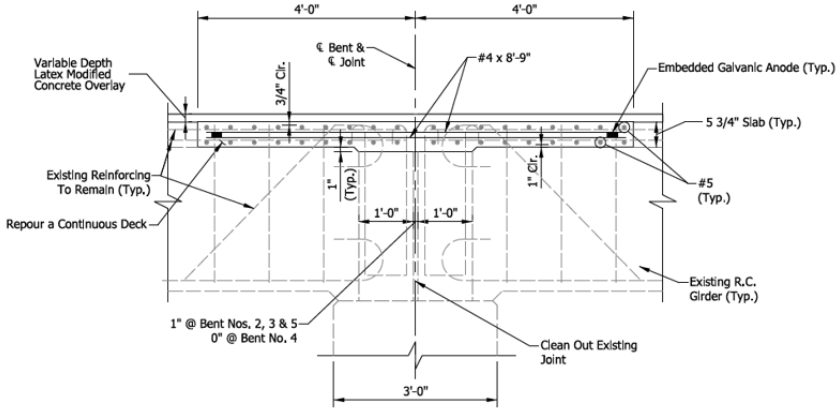

Figure 2.14: Link slab detail (SR 64 over SR 37)

According to the inspection report, the last visual inspection conducted was on December 20, 2016. Good condition was reported for the superstructure and substructure. Satisfactory condition with minor deterioration was reported for the deck and very good condition was reported for the wearing surface.

2.4.3 Owensville Road over I-64

According to the inspection report, the bridge rehabilitation was performed in 2015. Detailing of the link slab is shown in Fig. 2.15. This bridge has both steel and concrete girders. The rehabilitation using the link slab was performed over the piers where the steel and concrete girders meet. An overlay of latex modified concrete was used on top of the slab. The link slab detail is also a haunch type one.

A total of six inspection reports are evaluated between the years 2008 till 2018. Four inspection reports have been reported before the link slab construction, while two reports exist after the link slab construction. Although, the link slab was only added three years ago, the bridge seems to show increased deterioration by time as spalls are forming between the beams and the deck. Also, the deck is reported to have cracking in the lower surface after the link slab is added.

The last inspection to this bridge was performed on February 19, 2018. Good condition with some minor problems was reported for the superstructure, substructure, and wearing surface. Very good condition with some minor problems was reported for the deck. According to the report, during the rehabilitation in 2015 only the expansion joints over piers 2 and

4 were replaced with link slab. No joint was ever present over pier 3.

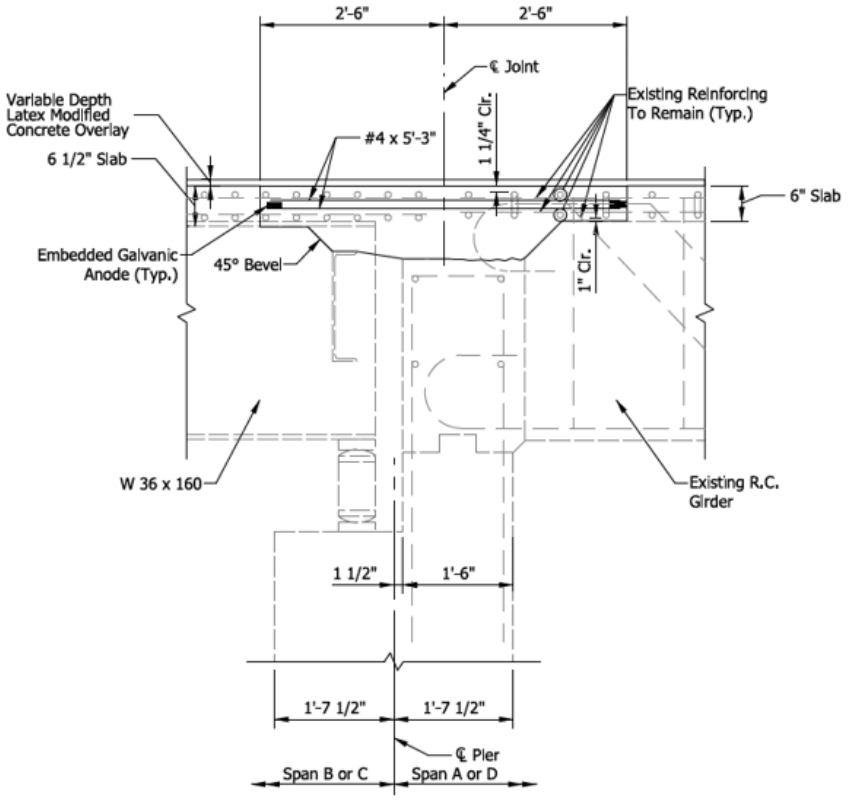

Figure 2.15: Link slab detail (Owensville Road over I-64)

2.4.4 SR-68 over I-64

According to the inspection report, the bridge rehabilitation was performed in 2015. Detailing of the link slab is shown in Fig. 2.16. This bridge consists of two intermediate continuous steel spans and two outer concrete spans. The rehabilitation eliminated the expansion joint at the connection between the steel and concrete spans using haunch type link slabs.

A total of seven inspection reports are evaluated between the years 2007 till 2018. Five inspection reports have been documented before the link slab construction, while two reports exist after the link slab construction. According to the inspection reports, the bridge was experiencing increased joint leakage over the years, which is eliminated now after the link slab installment. Furthermore, the link slab seemed to have no effect on the concrete girders. On

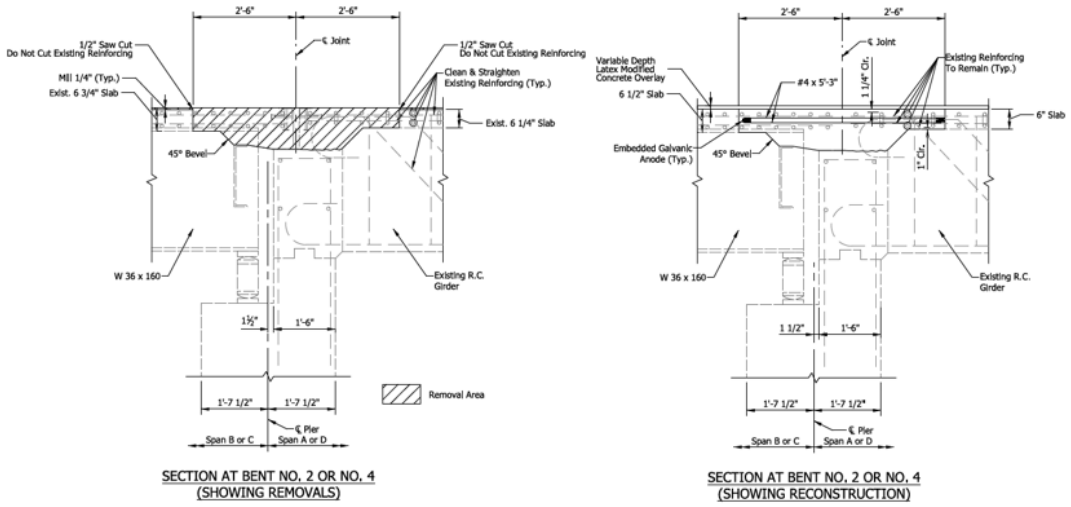

Figure 2.16: Link slab detail (SR 68 over I-64)

the other hand, the bridge showed increased deck underside cracking as well as consistent spalls in the deck at the interaction with the steel beams.

The last inspection to this bridge was performed on February 02, 2018. Satisfactory to good condition with some minor to moderate deteriorations was reported for the different bridge components in general: superstructure, substructure, and wearing surface. However, the deck underside surfaces exhibited numerous transverse cracking with light efflorescence. According to the report, during the rehabilitation in 2015 only the expansion joints over piers 2 and 4 were replaced with link slab. No joint was ever present over pier 3.

2.4.5 Hillcrest Road over US-50

According to the inspection report, the bridge rehabilitation was performed in 2017. Detailing of the link slab is shown in Fig. 2.17. This bridge consists of three intermediate continuous steel spans and two outer single concrete spans. The rehabilitation eliminated the expansion joint at the connection between the steel and concrete spans using debonded type link slab. It is worth noting that this bridge is the only debonded link slab bridge evaluated.

A total of seven inspection reports are documented between the years 2007 till 2017. Five inspection reports have been reported before the link slab construction, while only one report exist after the link slab construction. According to the inspection reports, the bridge seems to exhibit deterioration in the deck over time. However, as the link slab is recently installed and

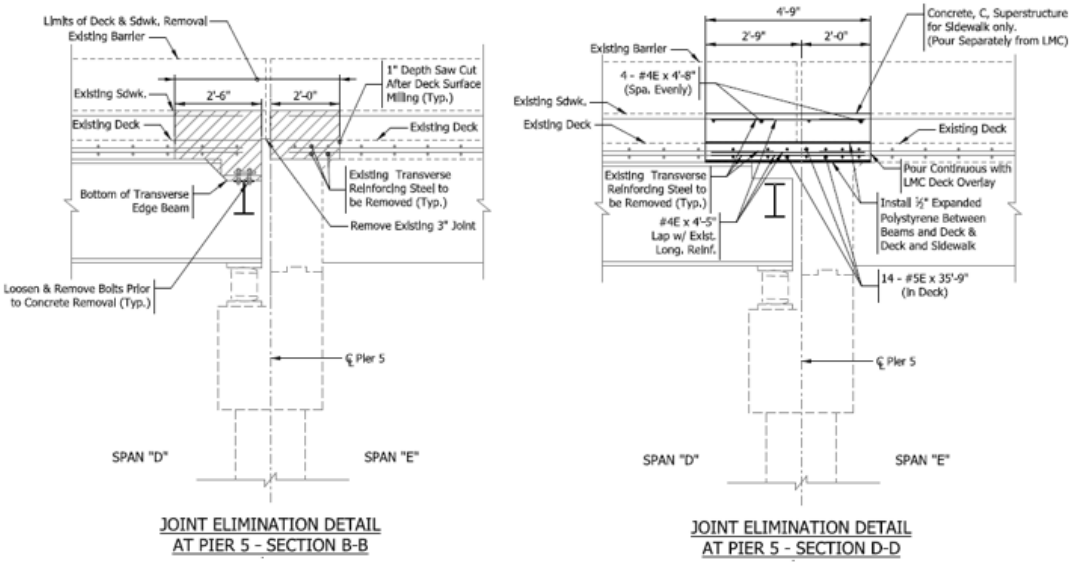

Figure 2.17: Link slab detail (Hillcrest Road over US-50)

there are not enough inspection reports after the link slab installment, it is difficult to assess the performance of the link slab.

The last inspection to this bridge was performed on November 01, 2018. Good condition was reported for both the superstructure and substructure, while satisfactory condition with minor deterioration is reported for the deck. The wearing surface is reported to be in excellent condition as the rehabilitation included changing the wearing surface. According to the report, during the rehabilitation in 2017 only the expansion joints over piers 2 and 5 were replaced with debonded link slab. No expansion joints were ever present over piers 3 and 4.

2.4.6 Summary of Inspection Reports

The detail for most of the link slabs identified in Indiana differ substantially than those in other states. The Indiana detail provides fully continuous deck that is achieved by having a continuous reinforcement through the bridge deck and the link slab. The concrete in the bridge deck near the expansion joints is removed to only leave the reinforcement in the section. The objective, then, is to have the link slab reinforcement going through the deck and being connected to the old reinforcement. Finally, the concrete is poured in the link slab and the bridge deck where the concrete was previously removed. The other important feature in the widely used detail in the state of Indiana is that no debonding is provided between the girders and the link slab. Consequently, the detail ensures the composite action between the

Figure 2.18: Cracking in Indiana link slab bridges as reported in inspection reports

girders and the deck through the fully bonded connection. It is important to note that only one bridge in the study is found to have a debonded link slab detail and that all link slabs studied are composed of normal strength concrete.

Although the assessment of the Indiana link slab bridges is based on a small number of bridges with no detailed scientific testing of these bridges, cracking of the bridges is observed in the inspection reports that can be attributed to the link slab construction. The cracking patterns reported in the inspection reports vary across the bridges ranging from shear cracking at the supports to cracking in the link slab causing leakage as shown in Fig. 2.18. Therefore, it is essential to assess the link slabs performance further and obtain more scientific data about the bridge conditions after the link slabs construction. However, most of the bridges reported transverse cracking in the bridge deck in the vicinity of the link slabs within the first year after the link slab construction. This observation is very dominant in the deck when

supported by steel girders. This observation is further investigated to identify its cause in subsequent chapters.

2.5 Summary of the Literature and Practice Review

Table 2.5 summarizes the literature presented in this synthesis. It can be seen from the table that link slabs are used mainly for rehabilitation purposes using steel bridge superstructure. Notice that the table specifies the type of link slab (i.e., haunched, flexible, and debonded) and the design detail used (i.e., details proposed by Caner and Zia [1998],Li et al. [2003], and Larusson et al. [2013]). Further, the research studies are classified into three major categories: experimental, analytical, and field work.

Table 2.5: Literature summary

Author	Research Objective	Type of Project	Girder Material	Connection Detail	FE Analysis	Laboratory Testing	Field Testing
Gastal [1986]	Develop FE program for continuous deck analysis	Rehabilitation/New	Steel/Concrete	NA	Yes	No	No
El-Safty [1994]	Determine optimum LS debonded length	Rehabilitation	Steel/Concrete	D-1	Yes	No	No
Caner and Zia [1998]	Investigate behavior of LS	Rehabilitation	Steel/Concrete	D-1	Yes	Yes	No
Caner et al. [2002]	Investigate LS seismic performance	Rehabilitation	Concrete	D-1	Yes	No	No
Li et al. [2003]	Investigate ECC application on LS	Rehabilitation	Steel	D-2	No	Yes	No
Li et al. [2005]	Investigate performance of ECC LS	Rehabilitation	Steel	D-2	No	No	Yes
Wing and Kowalsky [2005]	Assess LS performance	Rehabilitation	Steel	D-1	No	No	Yes
Okeil and El-Safty [2005]	Propose method for LS flexural anlalysis	Rehabilitation	Steel	D-1	Yes	No	No
Li et al. [2008]	Investigate causes of ECC LS cracking	Rehabilitation	Steel	D-2	Yes	No	Yes
Lam et al. [2008]	Discuss LS used by the MTO	Rehabilitation	Steel	H/F/D-1	No	No	Yes
Sevgili and Caner [2009]	Investigate of skew on LS seismic response	Rehabilitation	Concrete	D-1	Yes	No	No
Ulku et al. [2009]	Investigate LS behavior using FE	Rehabilitation	Concrete	D-1	Yes	No	No
Li and Saber [2009]	Investigate the use of FRP in LS	Rehabilitation	Steel	D-1	Yes	Yes	No
Aktan and Attanayake [2011]	Investigate effect of skew on LS	Rehabilitation	Concrete	D-1	Yes	No	Yes
Reyes and Robertson [2011]	Development LS with HPFRCC and GFRP	Rehabiliation	Steel	D-3	No	Yes	No
Larusson et al. [2013]	Development LS with HPFRCC and GFRP	Rehabilitation	Steel	D-3	No	Yes	No
Au et al. [2013]	Investigate LS long-term performance	Rehabilitation	Steel	D-2	Yes	Yes	Yes
Ozyldirim et al. [2017]	Investigate low-permeability FRCs with different types of fibers	Rehabilitation	Steel	D-2	No	No	Yes
Fu and Zhu [2017]	Investigate ECC mixtures for LS	Rehabilitation	Steel	D-1	Yes	No	No
Zheng et al. [2018]	Investigate behavior of LS with ECC and FRP reinforcement	Rehabilitation	Steel	D-2	No	Yes	No
Hou et al. [2018]	Investigate LS fatigue performance using UHDCC	Rehabilitation	Steel	D-2	No	Yes	No

Note: FE = Finite Element; NA = Not applicable; H = Haunched; F = Flexible; D = Debonded.
1 = Caner and Zia [1998].
2 = Li et al. [2003].
3 = Larusson et al. [2013].

Based on information collected for this synthesis, there are three different link-slab configurations: haunched, flexible, and debonded. The haunched and flexible configurations were used in Canada for deck rehabilitation during the early 1990s. Lam et al. [2008] indicated that it has been discontinued the use of these details because of their high costs as well as limitations in the girder end-rotations and girder depth. Presently, the debonded configuration is the most often used by DOTs in the United States and Canada. Debonded link slabs can be

full depth or partial depth. The depth refers to that of the reinforced-concrete deck. Therefore, a full-depth link slab is one that extends to the bottom of the bridge deck. Debonded link slabs can be either precast or cast-in-place concrete.

Typical design detail of a full-depth cast-in-place link slab is that proposed by Caner and Zia [1998]. This link slab has a debonded zone equivalent to 5% of each adjacent bridge span to reduce its stiffness and stresses, as illustrated in Fig. 2.1. A second full-depth cast-in-place link slab configuration was proposed by Li et al. [2003] to address the interfacial cracking problem observed in the Caner and Zia [1998] detail. This improved detail has a transition zone of 2.5% at each adjacent span in addition to the debonded zone of 5% (Fig. 2.3). This transition zone serves to move the interface away from the start point of the debonding. Example of a partial-depth precast link slab was proposed and tested by Larusson et al. [2013]. The configuration consist a 3 in thick link slab with a debonded zone of 6 ft and a transition zone at each 1 ft, as illustrated in Fig. 2.7.

Several materials have been used in the construction of link slabs. Link slabs can be constructed using conventional concrete. Example of acceptable field performance using traditional concrete has been documented by Wing and Kowalsky [2005]. Recently, DOTs have focused on developing advanced concretes that help both control cracking and minimize traffic disruptions. Virginia, Michigan, and New York are currently the pioneer agencies promoting the use of these materials for link slab applications. Advanced concrete materials used with link slabs include LMC, ECC, UHPC, and HyFRC [Fu and Zhu, 2017; Hou et al., 2018]. An alternative to traditional epoxy-coated reinforcement is GFRP [Reyes and Robertson, 2011; Larusson et al., 2013; Li and Saber, 2009]. Mix proportions of different concrete mixtures are given in Table 2.6. Reported properties of the GFRP reinforcement are presented in Table 2.7.

Leakage has been recognized as the primary cause of deterioration in link slabs. The use of low permeability and high durability concretes is highly recommended for the bridge systems [Ozyildirim et al., 2017]. The addition of fibers in the mixtures has been used to improve crack control and reduce the steel reinforcement ratio required in a conventional link slab [Lepech and Li, 2009; Zheng et al., 2018]. Other essential performance requirements for link-slab material selection are low drying shrinkage, high bond, and high early strength [Li et al., 2003, 2008].

The majority of link slabs in the United States are currently designed using the design methodology proposed by Caner and Zia [1998]. This procedure was developed based on approximate analysis methods and few tests conducted by the researchers [Gastal, F., and Zia, P., 1989; El-Safty, 1994; Caner and Zia, 1998]. Link slabs are designed to resist moments imposed by beam end rotations due to live load, and detailed with a debonded zone equivalent to 5%

of each adjacent bridge span to reduce stiffness and stresses. However, it has been reported that the design method is limited in accounting for the effect of axial forces on the link slab resulting from the girder end support conditions [Okeil and El-Safty, 2005; El-Safty and Okeil, 2008; Aktan et al., 2008]. Also, temperature loads are not considered for the calculation of the bending moments at the link slabs [Aktan et al., 2008; Ulku et al., 2009]. The design criteria adopted is the stress in the reinforcement that leads to overly conservative quantification of the amount of steel reinforcement [Lepech and Li, 2008, 2009].

Table 2.6: Mix proportions

Component [lb/yd^3]	**LMC**	**ECC**	**UHPC**	**HyFRC**
Cement	658	983	1200	490
Water	146	502	184	315
Fly Ash	-	1180	-	210
Silica Fume	-	-	390	-
Sand	1529	787	1720	1176
Coarse Aggregate	1232	-	-	1454
Ground Quartz	-	-	355	-
Latex	206	-	-	-
Accelerating Admixture	-	29	50.5	-
HRWR	-	-	51.8	-
PVA Microfibers	-	44	-	7.3
PVA Macrofibers	-	-	-	11
Polypropylene Microfibers	-	-	-	17.9
Steel Fibers	-	-	263	-

Note: LMC = Latex Modified Concrete; ECC = Engineering Cementitious Composite; UHPC = Ultra High Performance Concrete; HyFRC = Hybrid Fiber-Reinforced Concrete; PVA = Polyvinyl Alcohol; HRWR = High-Range Water-Reducing Admixture.

Table 2.7: Properties of GFRP reinforcement

Property	**GFRP**
Ultimate Strain Capacity [%]	2.4-2.8
Elastic Modulus [ksi]	46-48

Note: GFRP = Glass Fiber Reinforced Polymer.

Previous studies show that factors that directly affect the response of bridges with link slabs are: support conditions, debonded length, temperature gradients, concrete type, girder type, reinforcement ratio, interfacial bond strength, link-slab thickness, span-length ratio, girder height, and skew.

Chapter 3

Numerical Analysis of Indiana Bridge

The motivation of this chapter is to provide preliminary numerical analysis of an existing bridge in Indiana experiencing the typical cracking behavior observed in the inspection report to identify the causes for such observations. Consequently, to assess the performance of the common existing link slabs in Indiana, computational models are simulated on a selected bridge representing the bridge before and after the installation of the link slab. The bridge connecting the State Road 68 over the Interstate 64 is selected based on the analysis of the inspection reports presented in Chapter 2 to be a representative bridge. Other computational models are also analyzed for variations of the bridge to assess the effect of different parameters.

3.1 Bridge Model

The selected highway bridge was originally constructed in 1966. It was recently rehabilitated in 2015, when the link slabs were added to the bridge. This section provides a detailed description of the numerical modelling of the bridge before 2015 when it had expansion joints and after 2015 when these joints were eliminated. To model the existing bridge, SAP2000 software version 17 is used. The conducted analysis is a linear, elastic analysis with linear shape functions.

3.1.1 Geometry and Boundary Conditions

The bridge is a beam type bridge of length of 212′-4″ in total divided into four spans: two outer 46′-6″ concrete girders spans and two continuous inner 67′-8″ steel girders spans. The bridge superstructure is composed of six parallel girder axes 6 ft apart center to center 3 ft deep distributed over the width of the structure leaving 2′-3″ cantilever slabs on both sides. A 6.25 in deep concrete slab covers the whole super structure including the steel part with

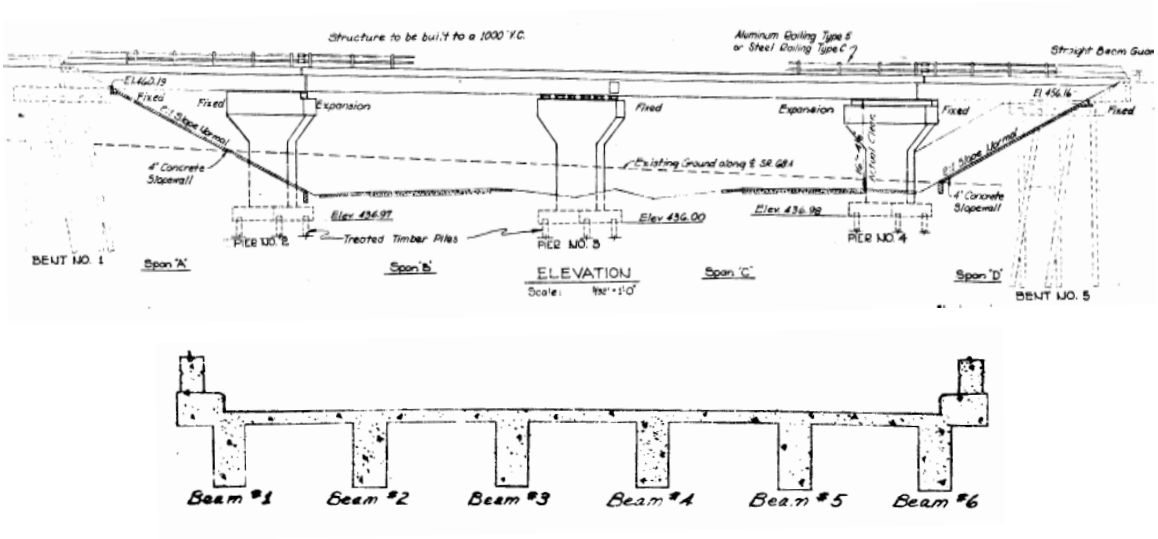

Figure 3.1: Bridge elevation and cross-section as reported in drawings

a skew angle of 47°. The bridge is supported on two abutments on the exterior, while the interior supports are concrete piers of variable cross-sections.

Only the superstructure of the bridge is modelled since the aim of the models is to assess the cracking observations in the superstructure. The substructure is represented by supports in the models. In addition, as the temperature is expected to be a crucial factor in the assessment of the link slab performance, the depth of the girders needed to be represented. Therefore, the girders are modelled using area elements to allow the variation of stresses and strains along the girders' depth. In this case, the concrete girders are modelled using thick shell elements of 1'-4" thickness. On the other hand, the steel girders are modelled by the combination of thick shell elements and frame elements. The shell elements represent the web of the girder, while the frame elements represent the girder flanges. The same modelling procedure applies for the steel and concrete diaphragms.

As per drawings, the concrete diaphragms are modelled only at the end of the concrete

Figure 3.2: Plan view of the girders and diaphragms of the bridge model

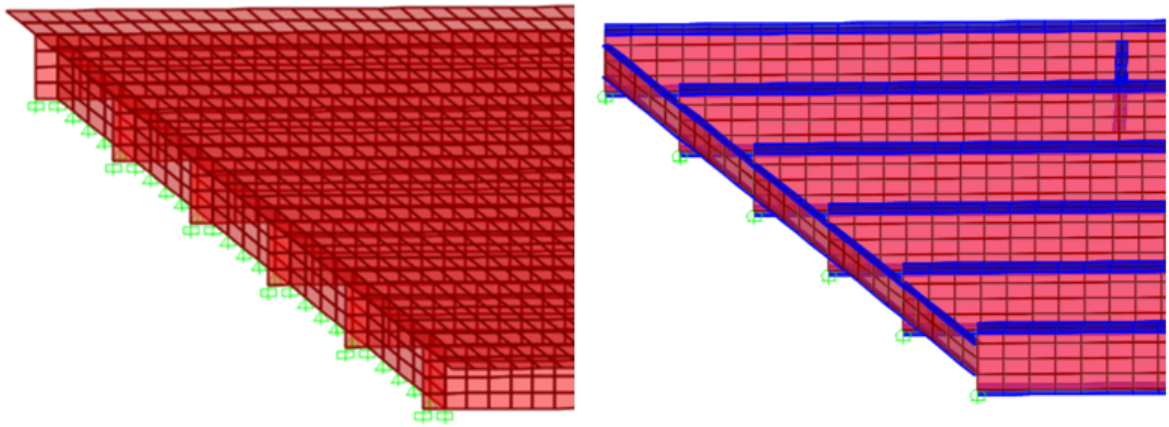

Figure 3.3: Boundary conditions for the concrete girders on the left and the steel girders on the right

spans parallel to the skewed angle. In contrast, intermediate steel diaphragms perpendicular to the longitudinal direction of the bridges are modelled in addition to end diaphragms in the skewed direction. The steel diaphragms are half the depth of the main girders and are aligned such that the center line of the diaphragm meets the center line of the main girder. The concrete slab is also modelled as thick shell elements of 6.25 in thickness. The slab is modelled continuous with the exception at the expansion joint locations in the model representing the bridge before the link slab installment. The connection between the slab and the girders is considered to transmit all straining actions and deformations in all models as the drawings indicate the existence of shear connectors between the steel girders and the concrete slab. Similarly, the link slab is considered fixed to the rest of the slab as the drawings show that the link slab is a haunched type detail where continuous reinforcement from the slab runs through the link slabs providing fixation.

According to the drawings, there is a shear key between the concrete diaphragms and the bridge substructure, which prevents the moment transfer between the diaphragms and the pier cap. Thus, the bottom of the concrete diaphragms is modelled as hinged. Although the substructure can theoretically have lateral deformations, the stiffness of the substructure is very high that replacing it with a support restraining motion would not introduce considerable error in the analysis. Unlike the diaphragms, the main concrete girders are fixed at the bottom ends as the drawings indicate that the substructure reinforcement goes through the girders.

In contrast, the steel diaphragms only connect the main steel girders with no connection to the substructure. Consequently, no restraints are needed on the steel diaphragms. Addition-

Concrete Structure		Steel Structure	
Slab	0.92′ x 1.35′	Slab	1.13′ x 1.35′
Girder	0.75′ x 0.92′	Girder	0.75′ x 1.13′
Exterior Diaphragm	0.75′ x 1.35′	Exterior Diaphragm	0.75′ x 1.35′
Link Slab	1.12′ x 1.35′	Exterior Diaphragm	0.75′ x 1.20′

Table 3.1: Mesh dimensions for concrete and steel structures

ally, the drawings show that the main steel girders are resting on bearings allowing horizontal movements. However, modelling all the supports as rollers would result in instability of the structure. To avoid that, the mid support is modelled as hinged, while the outer ones are modelled as rollers, which would lead to the same deformation behavior expected from the drawings.

Concrete girders and webs of the steel girders in the model are meshed to have four elements in the depth. The other direction is meshed to have aspect ratio in the range of 0.5 to 1, to avoid inappropriate elements that can cause numerical error. The resulting element sizes are presented in Table 3.1.

3.1.2 Loading

Since the aim of these models is to compare the bridge performance before and after the link slab construction, the different loading patterns are evaluated separately to assess the contribution of each loading case on the superstructure performance. Since the numerical analysis presented in this section is a linear elastic one, the effect of the combined loading is simply the addition of the results from the different load cases.

Since the link slab is installed as a rehabilitation process for the existing bridge, the link slab would not experience any dead load induced straining actions. Thus, the dead load is ignored in the models as it does not contribute to any cracking in the link slabs. The live load is assumed to be uniform load for the preliminary analysis. The uniform load is calculated by distributing the load of the H20-44 truck over its area. Three cases of live load are considered as follows:

1. The whole structure is loaded
2. Only the concrete structure is loaded
3. Only the steel structure is loaded

These live loads are selected such that the link slab would have either one of its adjacent spans is loaded or both are loaded simultaneously. All live loads are applied as distributed uniform

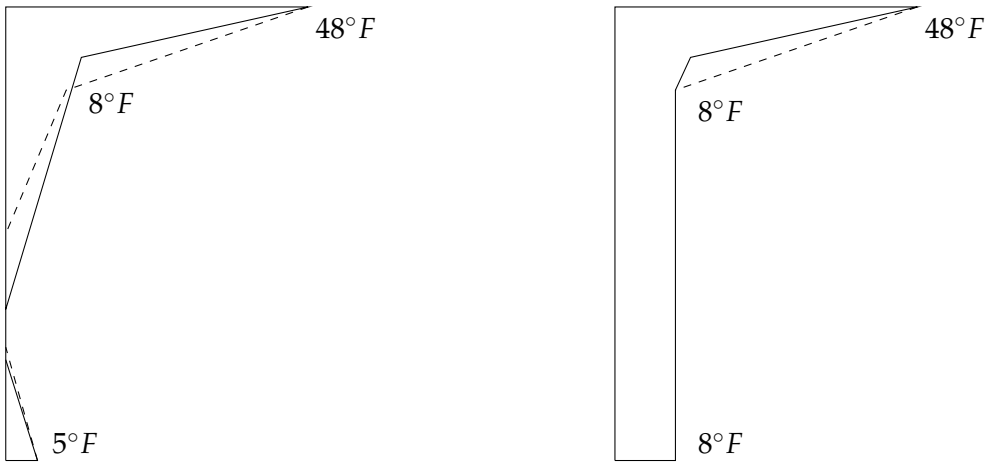

(a) Concrete Structure **(b)** Steel Structure

Figure 3.4: Applied (dashed) and AASHTO (solid) Gradient temperature diagrams for concrete and steel structures

load on the concrete slab in the gravity direction.

The temperature loading applied to the models is selected according to the AASHTO specifications [AASHTO, 2017]. The bridges are in Indiana, which is zone 3 as specified in the code. Thus, assuming the structure is built in a moderate temperature, two uniform temperature loadings are considered a +35° F and a -45° F temperatures. The uniform temperature is applied on all members existing in the model whether frame or shell element.

Gradient temperature loadings are also considered following the AASHTO specifications. Again, using the specifications for zone 3, the concrete gradient temperature diagram is shown in Fig. 3.4. SAP2000 assumes linear functions within the element. However, the elements nodes do not coincide with the points of changing slopes in the diagram in Fig. 3.4. Therefore, a minor approximation in the loading is introduced by calculating the exact values of the temperature at the elements' nodes location and assuming a linear change between these values creating a piece-wise linear approximation diagram with the maximum and minimum matches the original diagram. On the other hand, the steel gradient temperature diagram is different from the concrete as shown in Fig. 3.4. To apply this diagram, the concrete slab is subjected to a gradient temperature, while the steel girders are subjected to uniform temperature of 8°F. Moreover, the same approximation procedure applies in the steel structure due to the mismatch between the elements' nodes and the points of changing slopes in the diagram.

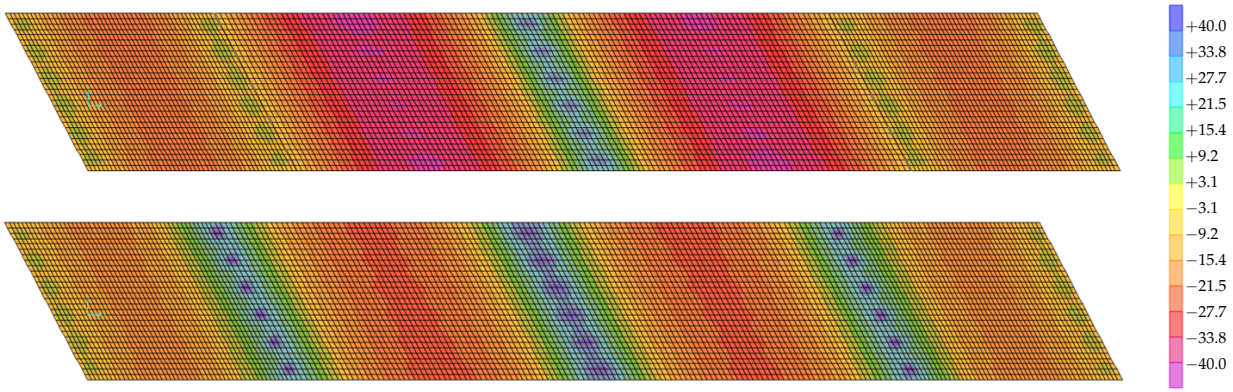

Figure 3.5: Axial forces (kips) in the slab due to fully loaded structure under live load. The top figure is the bridge with expansion joint. The bottom figure is the bridge with link slabs

3.2 Results

This section discusses the results of the original two models. The analysis of the different loading conditions on the bridge has shown that the slab primarily experiences stresses in the longitudinal direction only. The transverse direction straining actions are negligible and, hence, can be neglected. In addition, the super structure seems to behave as a composite structure where the slab acts as a flange to the girders experiencing axial stresses.

The analysis of the live load cases indicates that the fully loaded structure represents the critical case of the three cases of live loads. The link slab model shows a redistribution of the moments as the slab has become continuous with the addition of the link slab. Although, the girders do not exist below the link slab, the link slab is observed to provide continuity between the girders. Consequently, tensile stresses are observed in the slab at areas of negative moments, while compressive stresses are observed in the areas of positive moments. The results show negative moments at the lines of supports in the link slab, where as almost zero moments are present at the same locations in the model with no link slab due to the existence of expansion joints as shown in Fig. 3.5. Due to the redistribution of stresses from the link slabs installment, the stresses are reduced in the link slab model compared to the model with the expansion joints.

The results also show that the link slab not only provides continuity to the slab but also continuity to the main girders. According to the axial forces results, the slab acts like a flange to the girders. The slab experiences tension stresses at the lines of supports in the link slab models, while it experiences almost zero stresses at the expansion joints in the model with no link slab. Therefore, the results indicate that the bridge performs better with the link slab

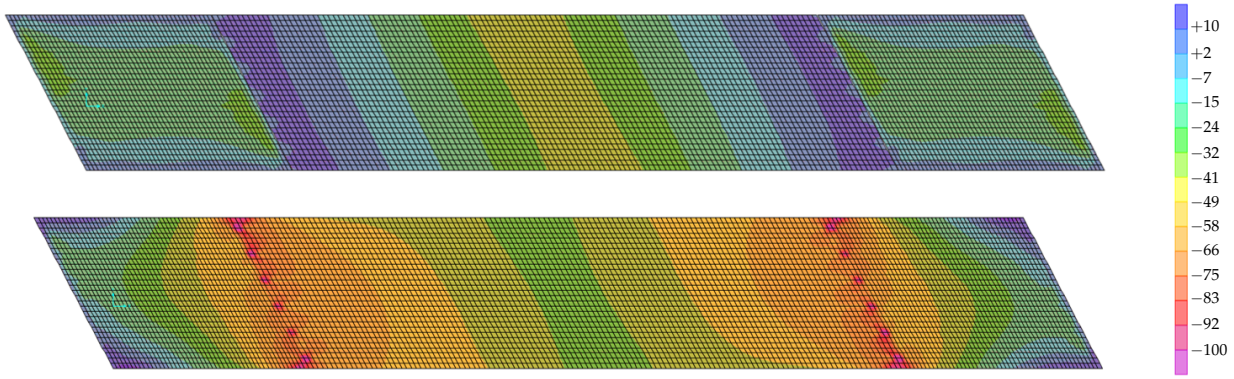

Figure 3.6: Axial forces (kips) in the slab due to uniform increase in temperature. The top figure is the bridge with expansion joint. The bottom figure is the bridge with link slabs

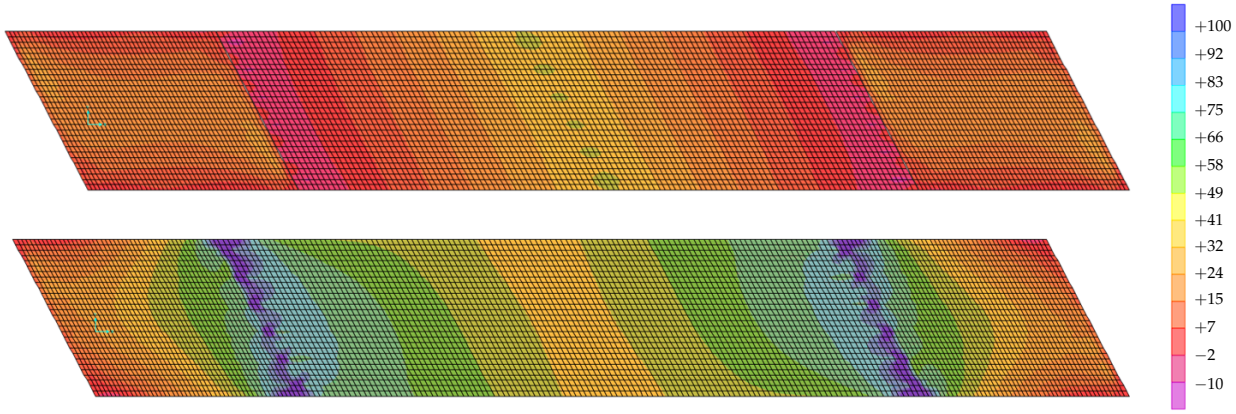

Figure 3.7: Axial forces (kips) in the slab due to uniform decrease in temperature. The top figure is the bridge with expansion joint. The bottom figure is the bridge with link slabs

installed than the bridge with expansion joints under live load.

Unlike the live load analysis, the uniform temperature analysis shows that the link slab bridge exhibit significantly higher axial stresses in the slab compared to the bridge with the expansion joint in both uniform temperature cases as shown in Figs. 3.6 and 3.7. This result is reasonable as the link slab prevents the bridge from deforming with temperature variation causing stresses in the slab. The results show high tensile stresses in the case of the temperature reduction which is way above the cracking limit (more than thrice) while almost the same magnitude compressive stresses are observed in the temperature elevation case which can be easily accommodated by the concrete strength.

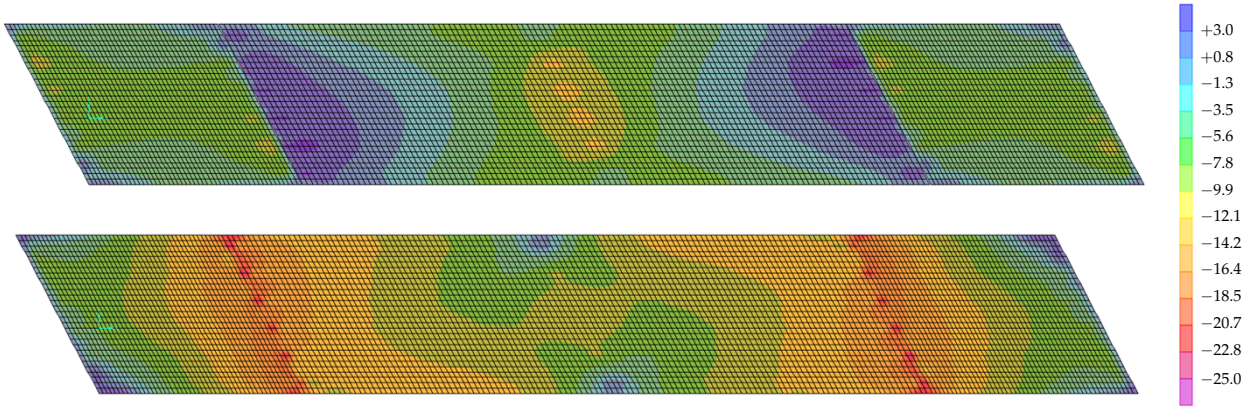

Figure 3.8: Axial forces (kips) in the slab due to gradient temperature. The top figure is the bridge with expansion joint. The bottom figure is the bridge with link slabs

It is important to note that the uniform temperature analysis assumes that the link slab is constructed in a moderate temperature climate. In other words, if the link slab is constructed on elevated temperature days, the bridge would experience higher tensile stresses than presented here, while constructing the bridge in winter would significantly reduce the tensile stresses on the expense of compressive stresses resulting from the elevated temperature case.

The final loading case considered for these models is the gradient temperature loading case. The results from this case of loading show similar behavior to the elevated uniform temperature. However, the overall values from the gradient case is much less than the uniform case (almost quarter). Consequently, this load case is far from critical for the evaluation of the link slab performance as the bridge in this case experience very low compressive stresses that do not contribute to the bridge cracking.

It can be concluded from the analysis of these two models is that the bridge cracking reported in the inspection reports is mainly due to the decrease of temperature between the summer and the winter leading to the cracking observed in the first year after the link slab construction. The cracking observed coincides with the stress concentrations observed in the model as the cracking is in the slab near the link slab locations.

3.3 Parametric Study

Several Models that are variations of the bridge are created to test the effect of different parameters on the performance of the link slab in the bridge. Two sets of models are created

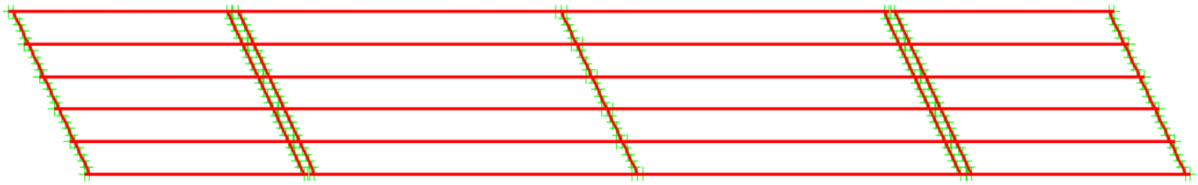

Figure 3.9: Plan view of the girders and diaphragms of the bridge model where all girders are made of concrete

for this section to test the effect of the boundary condition and the interaction between the steel and concrete on the bridge performance. The first set of models is to evaluate the effect of having a concrete structure only compared to the mixed one. The second set of models aims to evaluate the effect of boundary conditions on the stress distribution in the bridge.

3.3.1 Effect of Material

An explanation to the results from the previous section that show the high effect of the uniform temperature on the stresses in the slab is the difference between the expansion coefficients of the concrete and steel. This difference causes a differential strain between the steel and concrete that can lead to high stress concentration at the connection interface. Consequently, a variant of the bridge is modelled by replacing the steel girders in the model with concrete ones to check if these high stresses would be reduced. The new concrete girders are selected to match the concrete girders previously modelled. The boundary conditions and the diaphragms are also selected to match those in the concrete part of the bridge. To do so, interior diaphragms are removed, while the external ones are replaced with concrete ones resting on hinge supports. Furthermore, the roller supports are replaced with fixed ones as shown in Fig. 3.10.

The results of this analysis show that there is no difference in the distribution of the stresses due to live load. However, as expected, the distribution of stresses due to temperature loading significantly changed from the original bridge. The magnitude of the maximum stresses due to the uniform temperature in the bridge variant is less than the maximum of the original bridge. In contrast, high stresses are observed over wider area in the slab in the variant model compared to the original bridge. Note that in both models the bridge is completely restrained against any longitudinal expansion or deformation. The difference can be attributed to the difference between the modulus of elasticity of concrete and steel.

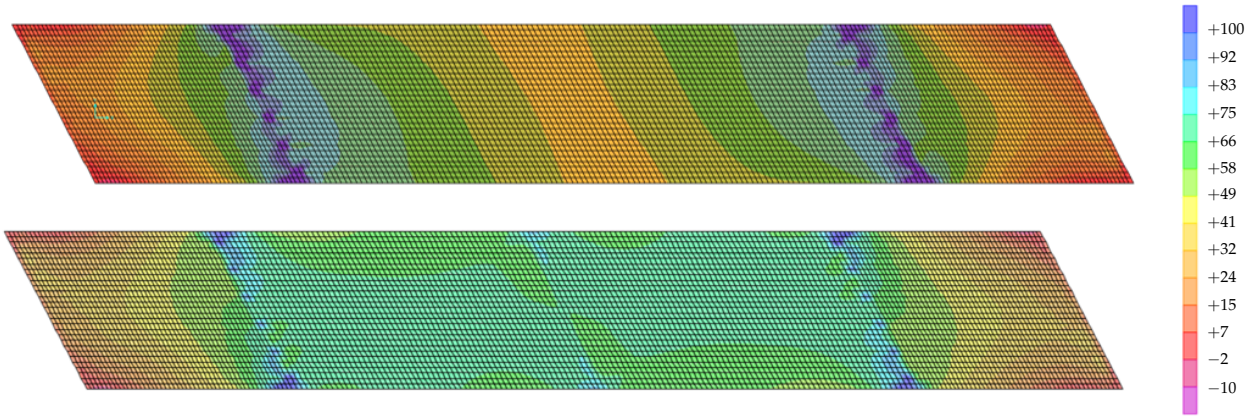

Figure 3.10: Axial forces (kips) in the slab due to uniform decrease in temperature. The top figure is the original bridge with link slab. The bottom figure is the bridge variant (All concrete girders) with link slab

3.3.2 Effect of Boundary Conditions

One of the important factors reported in literature that affects the performance of the link slab bridges is the boundary conditions at the supports of the structure. Thus, different models are created to assess the effect of the boundary conditions. In this analysis, three different cases from the original bridge are considered:

1. The first model changes the fixed boundary conditions at the concrete part of the bridge to hinged supports (i.e., HHRHRHH). This model represents the structure with the shear key passing through the main girders as well.

2. The second model replaces the same supports along with the concrete diaphragms supports with rollers (i.e., RRRHRRR). This represents the structure if all supports are bearings allowing horizontal movements.

3. The third model has the same boundary condition as the second one with the addition of supports at the end of the bridge slabs that restrains movement in horizontal direction. This model represents the bridge if all supports are bearings allowing horizontal movements without expansion joints at the abutments. This can be due to the introduction of link/approach slabs in this joint.

The results from the live load analysis show a significant decrease in the stresses at the link slabs in all three aforementioned models on the expense of higher tensile stresses at the middle support compared to the original bridge model with link slab. This can be attributed to the fact that releasing the moment from the supports at the link slab reduces the stiffness causing redistribution of stresses to increase in stiffer areas and reduced at the link slabs. This

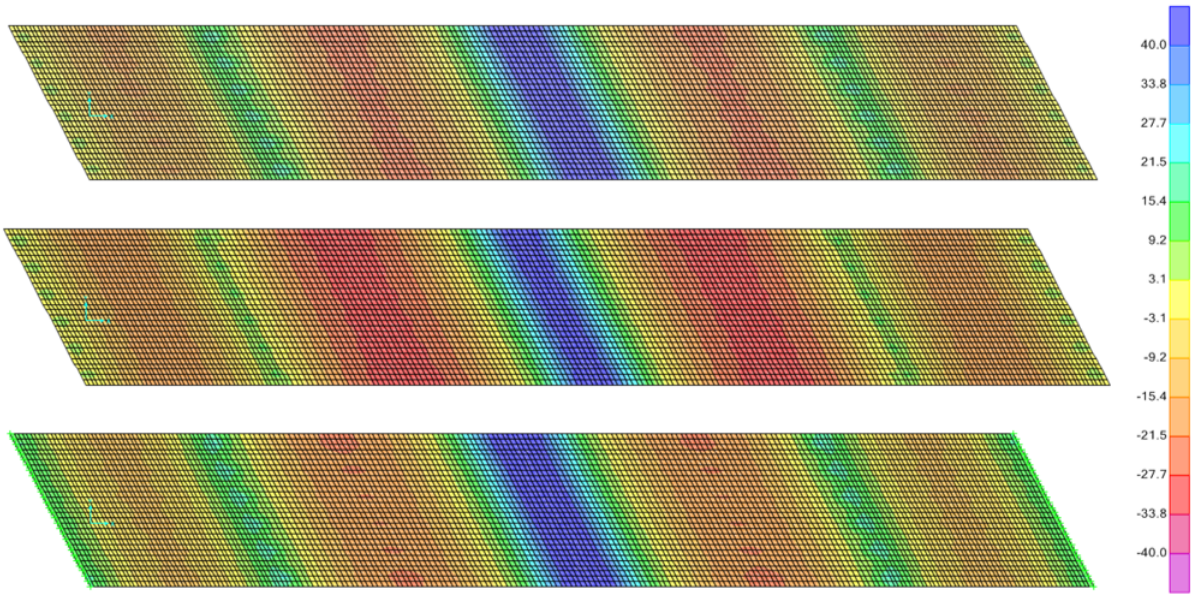

Figure 3.11: Axial forces (kips) in the slab due to fully loaded structure under live load. The top figure is the bridge with HHRHRHH support configuration. The middle figure is the bridge with RRRHRRR support configuration. The bottom figure is the bridge with RRRHRRR support configuration and supports representing approach slab

is, also, visible in the third variant model as more tensile stresses is observed at the new supports added. The second model with all roller supports seem to have the highest compressive stresses (positive moments) in the slab in the steel spans.

Additionally, the live load results show that the stresses in the link slab is almost equivalent to the stresses in the slab around the expansion joint in the original bridge when it had the expansion joints. It can, then, be deduced that the installment of the link slabs provides stiffness equivalent to the stiffness induced by adding the moment restrains (fixation) at the supports at the expansion joints. Although the values of the three variants seem to suggest that all stresses are below the cracking limit, the results shown here are considered averaged as the slab is modelled using area elements showing uniform axial stresses. The stress values at the top and bottom fibers can increase compared to these values.

The uniform temperature results show wide variations in the stresses between the three variants. The first variant, where the fixed supports are replaced with hinged supports shows almost no difference in uniform temperature results from the original bridge with link slabs results. On the other hand, the second variant shows almost no stresses due to temperature. This is reasonable as the support condition arrangement allows the structure to expand at the

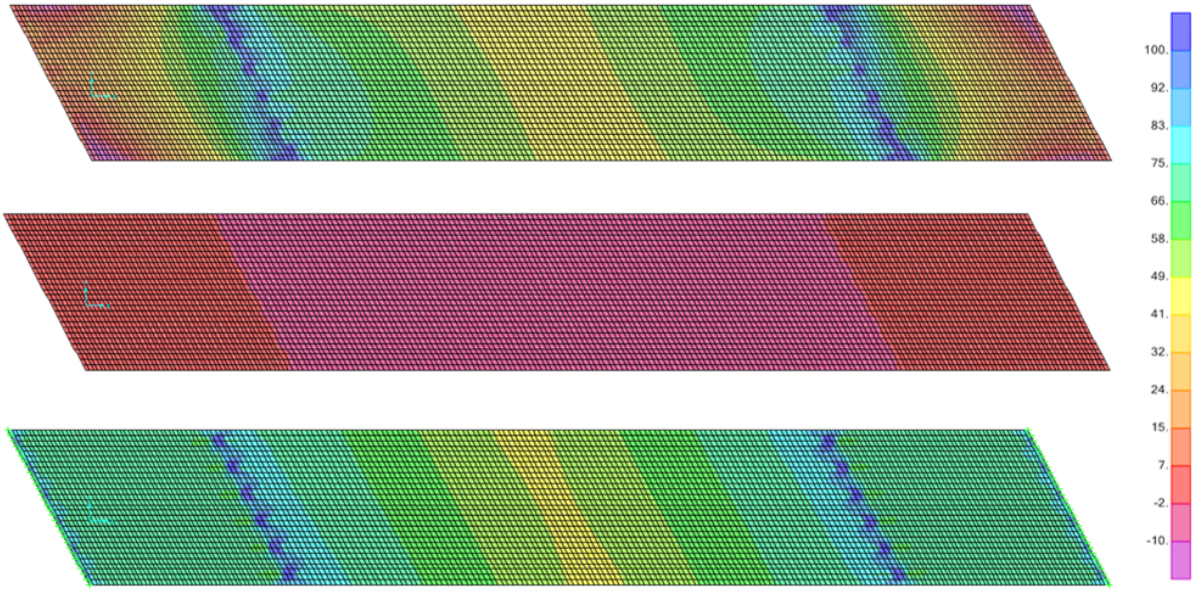

Figure 3.12: Axial forces (kips) in the slab due to fully loaded structure under live load. The top figure is the bridge with HHRHRHH support configuration. The middle figure is the bridge with RRRHRRR support configuration. The bottom figure is the bridge with RRRHRRR support configuration and supports representing approach slab

ends of the bridge causing no induced stresses all over the bridge. However, connecting the ends of the bridge to the approach slab or abutments without allowing expansion produces stresses that are even higher than the original arrangement in general. The steel structure results in these two models seem not to vary much, but the concrete part show significant change in the stress distribution. The variant model, where the slab is connected to the approach slab show significant increase in the tensile stresses in the concrete structure compared to the original model since this connection prevents the expansion at the ends of the bridge as shown in Fig. 3.12.

These results show that the stresses in the bridge due to both live load and temperature are highly sensitive to the boundary condition configuration. The high stresses due to temperature can be completely removed if the structure is allowed to expand which in turn would greatly reduce the demand on the link slab. This could then lead to reduction in the cracking observations and increase the link slab performance.

Chapter 4

Bridge Parameter Investigation

In order to evaluate the effect of factors on the behavior of link slabs identified from the literature review, a preliminary investigation is conducted using a series of 3D finite element models developed using the Abaqus/CAE software. This software is selected because of the advantages offered to solve contact problems. The primary focus of the investigation is to evaluate the effect of support conditions and debonded length on the stress distribution and potential crack initiation in link slabs. Each variable is investigated separately to isolate its effect.

Two bridge structures are investigated in this study. The bridge structures are based on the Michigan bridge studied by Aktan et al. [2008], but with a rectangular cross-section. The first structure (Case 1) represents a bridge structure rehabilitated using link slabs. It consists of a 1670 in bridge with two equal 834 in spans and zero skew, connected by a link slab. The superstructure consists of a single line of concrete girders with an effective flange width of 76 in. Deck thickness is 9 in. Fig. 4.1 shows the layout and the cross section of the bridge deck link slab. A second bridge structure (Case 2) with the same geometrical and material properties, but with a continuous and fully bonded deck, is used for comparison purposes (Fig. 4.2). This structure simulates new bridge construction.

Table 4.1: FEM material properties

Material	Young's Modulus [ksi]	Poisson's Ratio	Thermal Coefficient [in/in/F]
Concrete	4031	0.2	6.0e-6

All components of bridge superstructure are modeled with same material using solid brick elements with linear elastic properties. Table 4.1 shows the material properties used in the

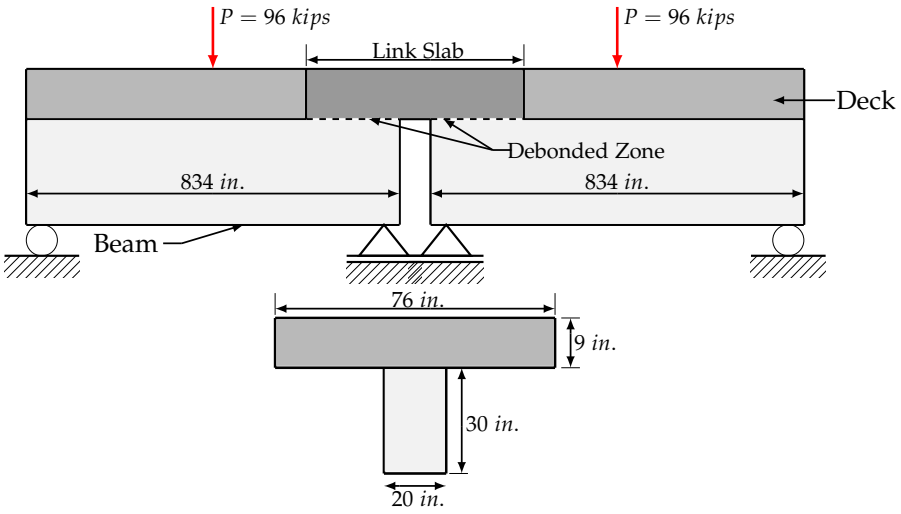

Figure 4.1: Bridge deck link slab (Case 1)

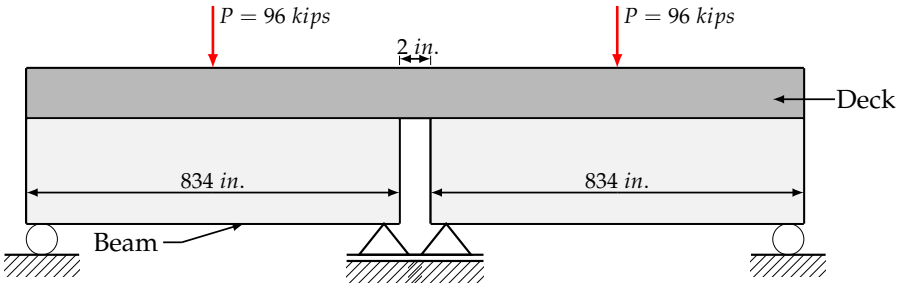

Figure 4.2: Continuous bridge deck (Case 2)

models. None of the models incorporates the steel reinforcement. It is assumed that all parts, except for the girder ends at the joint location, are fully bonded. Therefore, tie constraints are used to model the full composite action between the concrete deck and girder as well as at the interface between the concrete deck and link slab (Fig. 4.3). Table 4.2 presents the master and slave surfaces used to define the constraints in the models. Contact properties are used to model the debonded zone at the link slab region. A mesh size of 2.5 in is used for all elements.

The supports are placed as a line of nodes at the bottom of each beam end and are modeled by constraining the appropriate degrees of freedom (Fig. 4.4). A fixed support (F) is represented as a node with all displacements and rotations restrained. A hinged support (H) is defined by constraining the displacements in all three directions. A roller support (R) is modeled by constraining both vertical and transverse displacements.

Table 4.2: Surfaces for tie constraint definition

Constraint	Master Surface	Slave Surface
1	Top girders	Bottom decks
2	Deck sides	Link slab sides

The models are subjected to the action of two different loadings: live load and uniform temperature load. Live load is applied statically as a concentrated load at the middle of each span, as shown in Figs. 4.1 and 4.3. Each concentrated load equivalents to the resultant of a design truck (H20-44) times an impact factor of 1.33. The two concentrated loads are applied by using cylinders to distribute the load uniformly along the effective width, as illustrated in Fig. 4.3. These cylinders are idealized as rigid bodies to ensure deformations only on the bridge structure. The uniform temperature load considered is -50 °F (Zone 3 according to the AASHTO specifications [AASHTO, 2017]). This negative uniform temperature load is selected because produces, for most cases, high tensile stresses on the link slab. The uniform temperature is applied on all members existing in the model. The thermal coefficient of expansion for concrete are given in Table 4.1. As the link slab is installed for bridge rehabilitation purposes, the dead load can be ignored in the models because it does not contribute to link slab cracking.

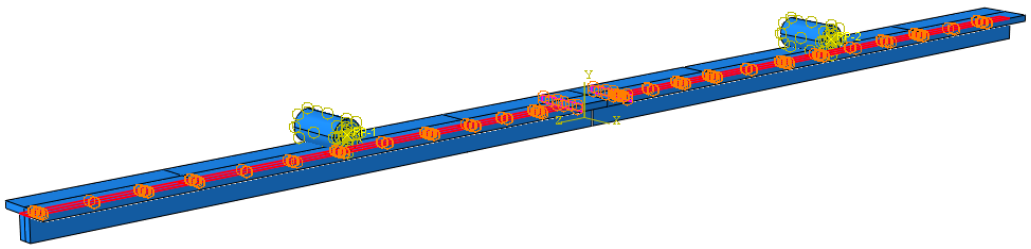

Figure 4.3: Tie constraint locations

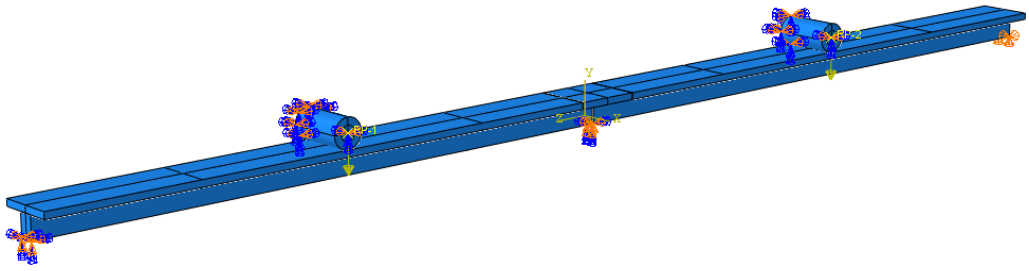

Figure 4.4: Model assembly for live load

4.1 Effect of Support Conditions

Seven different combinations of girder support restraints are considered in this study: FFRH, HHHH, HRHH, HRRH, HRRR, RHHR, and RRHR. These support arrangements are selected because some of them represent the practice in Indiana and others are previously identified from the literature. Figs. 4.5 and 4.6 show the longitudinal normal stresses measured at the top of the link slab when the bridge structure is subjected to live load and uniform temperature load, respectively. Notice that both figures show the stresses for only the link slab region. For all support cases shown in these figures, the length of the full-depth link slab is kept constant as 43 in at each side from the axis of symmetry over the gap. This length is equal to 5% debonding. It can be seen from the figures that the behavior of link slabs is affected by the bridge boundary conditions. Fig. 4.5 shows that higher longitudinal normal stresses on the link slab under live load are produced for those support arrangements with roller support below of the link slabs (i.e., support cases RRHR, HRRH, FFRH, and HRHH). Fig. 4.6 shows that, as the structure is more restrained at the outer supports, higher longitudinal normal stresses are observed due to uniform thermal load (i.e., support cases HRRH, FFRH, HRHH, and HHHH). Tables 4.3 and 4.4 show the comparison between the two bridge cases considered in this study when the beam model is subjected to live and thermal loads, respectively. The results presented in Table 4.3 show that using a link slab with a debonded length of 5% at each span decreases the stresses due to live load around 38% for all support cases when comparing the results from those of a continuous and fully bonded deck (0% debonding). For the uniform temperature load case, the results of Table 4.4 show that the effect of 5% debonding was negligible for all support cases except one. For HHHH, no thermal release was available and the thermal gradient resulted in an increase of 26% compared with the continuous and fully bonded deck. Notice from the information presented that changing position of H support does not produce any difference on the link slab response for both live and thermal loads (i.e., stresses for support cases RRHR and HRRR are the same). Due to symmetry in the model, stresses in the link slabs remained the same when having fixed (i.e., FFRH) or pinned supports (i.e., HRHH) at the ends under the loadings cases considered.

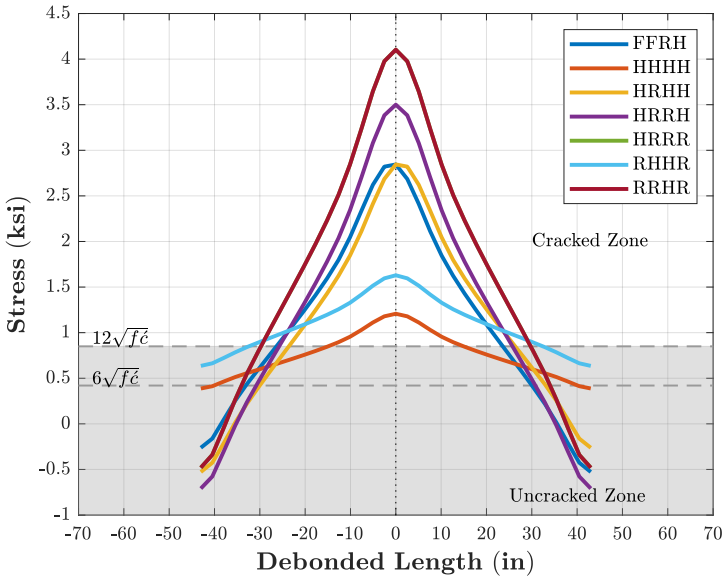

Figure 4.5: Effect of boundary conditions under live load

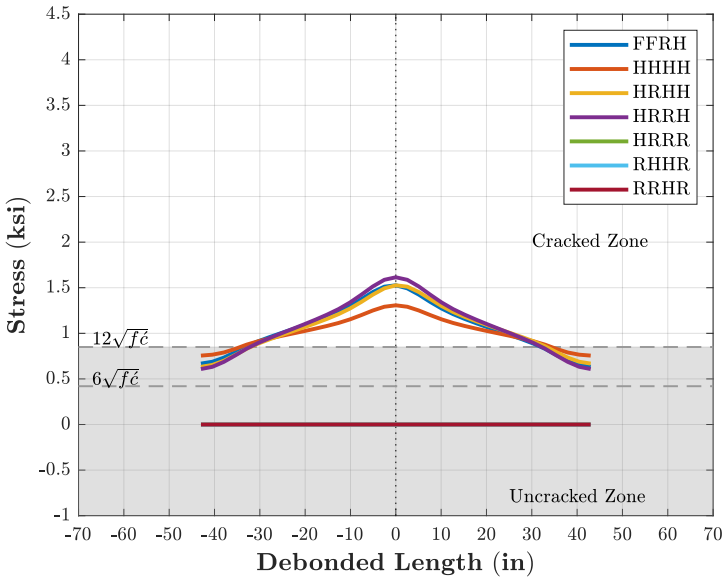

Figure 4.6: Effect of boundary conditions under uniform temperature load

Table 4.3: Maximum stresses at top of link slab due to live load

Support Conditions	Max. Stress [ksi]		Difference [%]
	Case 1	Case 2	
FFRH	2.90	5.02	-42
HHHH	1.21	2.09	-42
HRHH	2.90	5.02	-42
HRRH	3.52	5.82	-40
HRRR	4.13	6.44	-36
RHHR	1.64	2.37	-31
RRHR	4.13	6.44	-36

Note: F = Fixed.
H = Hinged/Pinned.
R = Roller.

Table 4.4: Maximum stresses at top of link slab due to uniform temperature load

Support Conditions	Max. Stress [ksi]		Difference [%]
	Case 1	Case 2	
FFRH	1.53	1.48	4
HHHH	1.31	1.04	26
HRHH	1.53	1.48	4
HRRH	1.61	1.64	-2
HRRR	0.00	0.00	0
RHHR	0.00	0.00	0
RRHR	0.00	0.00	0

Note: F = Fixed.
H = Hinged/Pinned.
R = Roller.

4.2 Effect of Debonded Length

The length of the debonded zone is varied to investigate its effect on the behavior of link slabs. The following debonded lengths at each adjacent span are investigated: 9, 18, 26, 36, 42, 51, and 61 in. These lengths expressed in terms of the span length correspond to the following percentages: 1, 2, 3, 4, 5, 6, and 7. The beams are subjected to live and thermal loads separately. Figs. 4.7 and 4.8 illustrate the effect of of varying the debonded length when the

bridge is subjected to live load. Figs. 4.9 and 4.10 illustrate the effect of varying the debonded length when the bridge is subjected to uniform temperature load. Notice that in all figures the results are presented for only the link slab region and for each support arrangement. The longitudinal normal stresses are measured at the top of the link slab. It can be seen from the results that increasing the debonded length, when the bridge is subjected to live load, results in reduced longitudinal normal stresses for all the boundary conditions considered. Bridges that allow thermal expansion experience no stresses in the link slab. For all boundary conditions considered, stresses due to live load are approximately three times greater than those observed due to temperature loads.

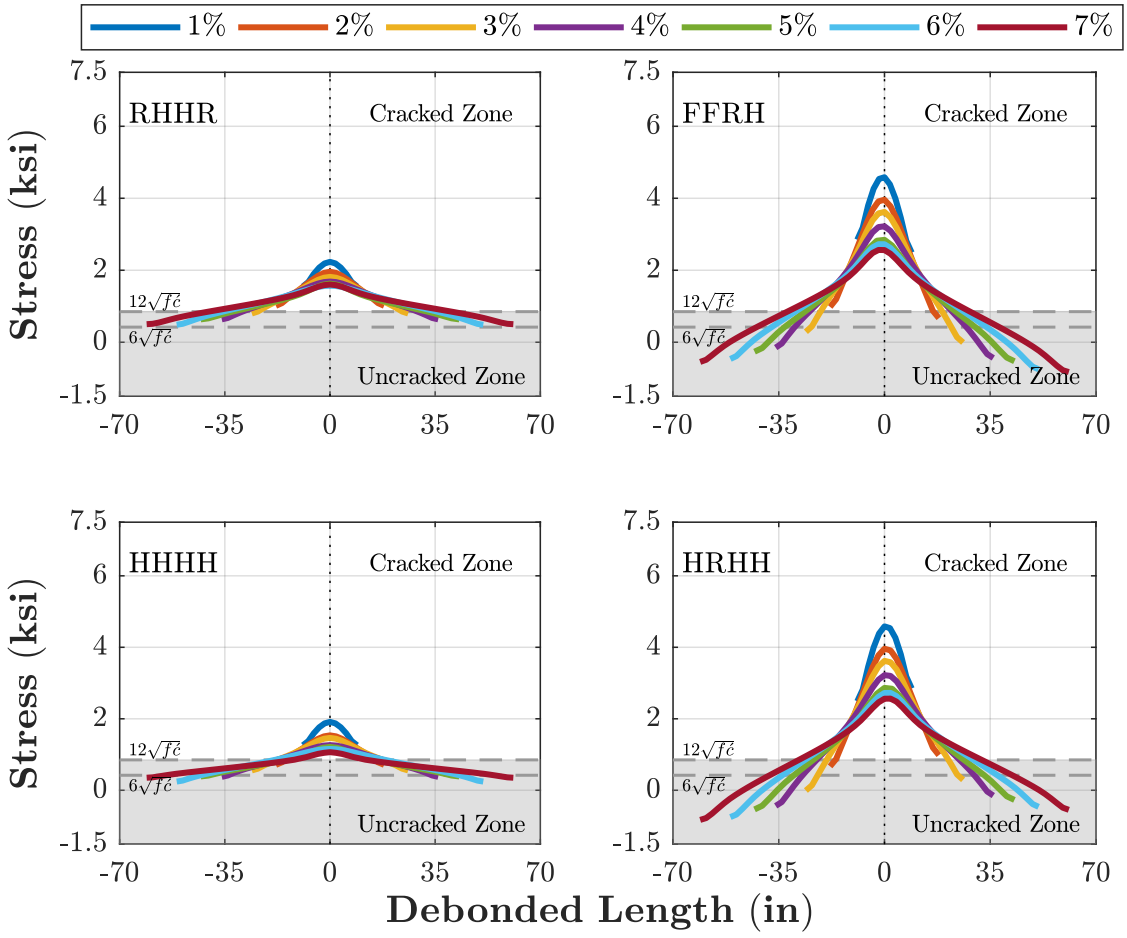

Figure 4.7: Effect of debonding under live load for support conditions: RHHR; FFRH; HHHH; and HRHH

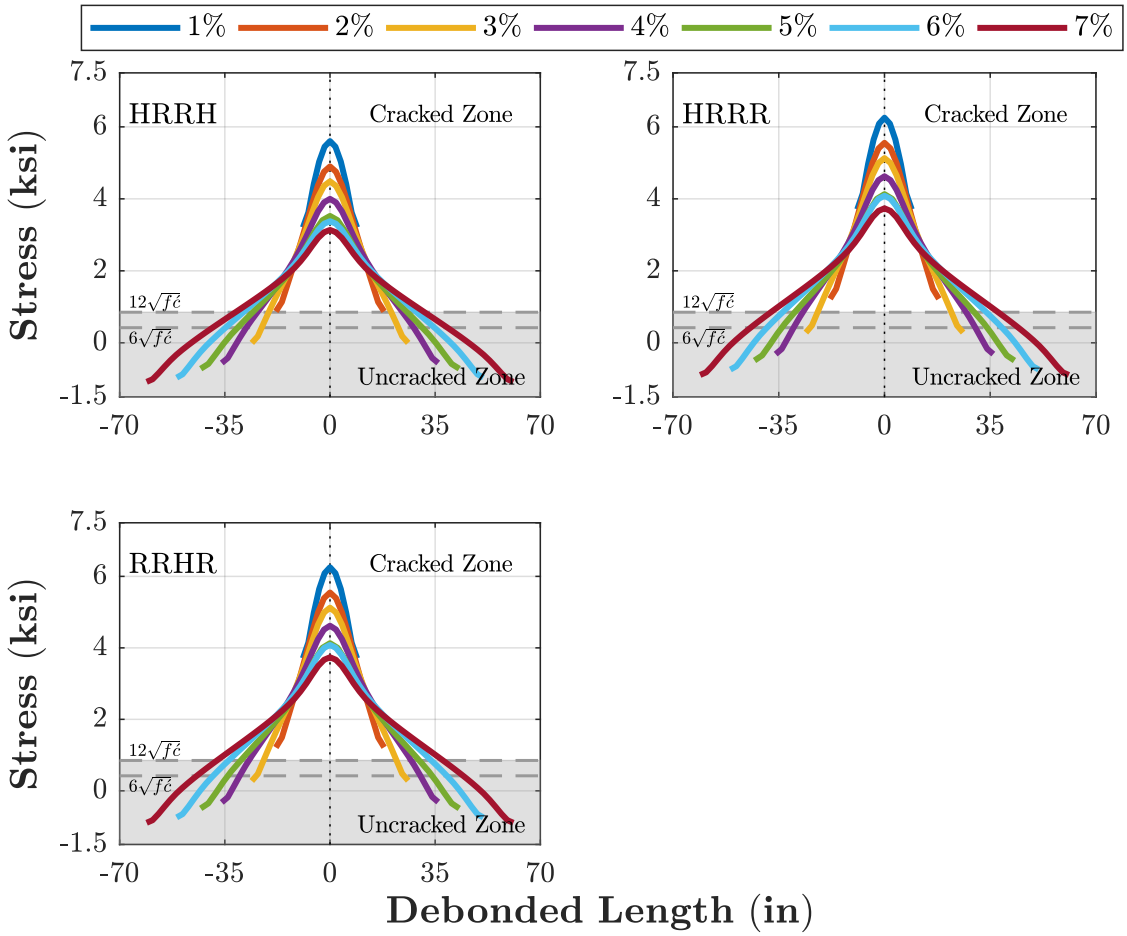

Figure 4.8: Effect of debonding under live load for support conditions: HRRH; HRRR; and RRHR

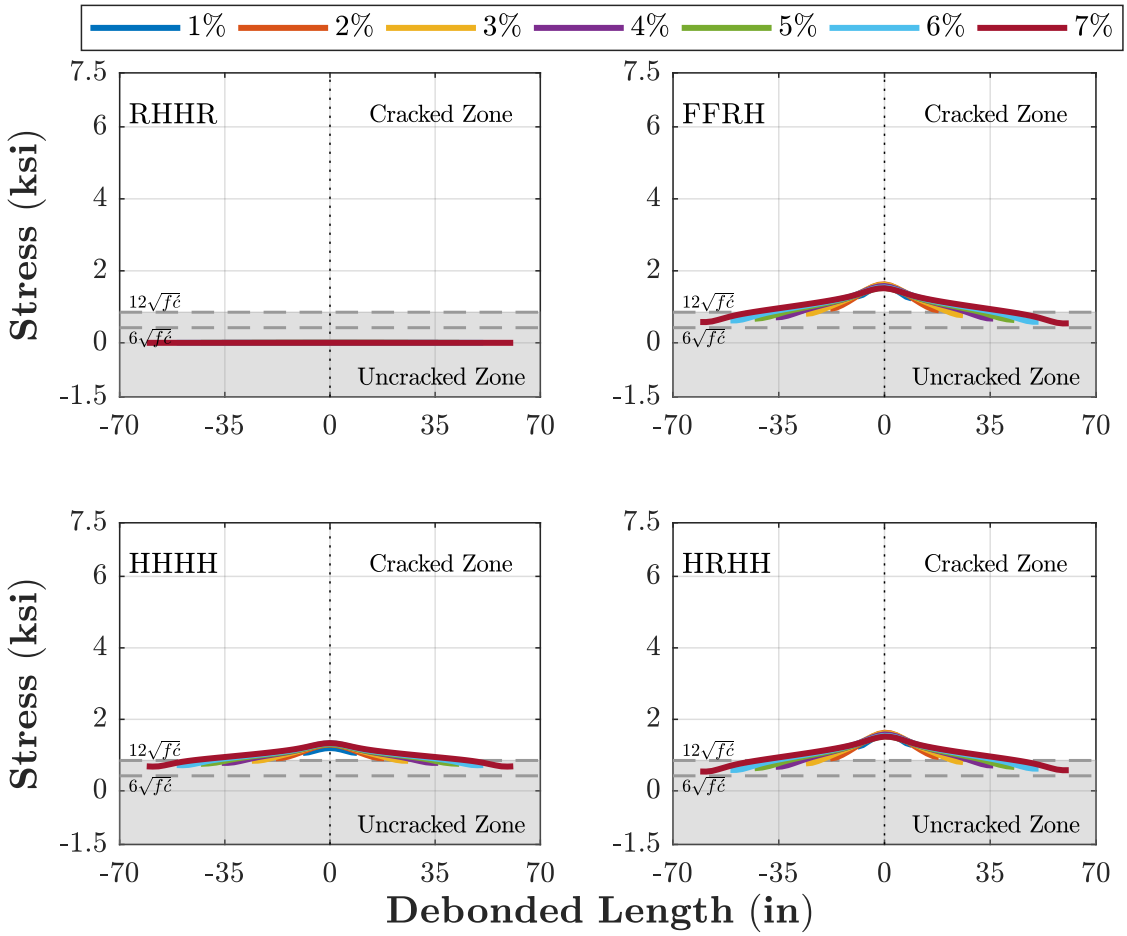

Figure 4.9: Effect of debonding under uniform temperature load for support conditions: RHHR; FFRH; HHHH; and HRHH

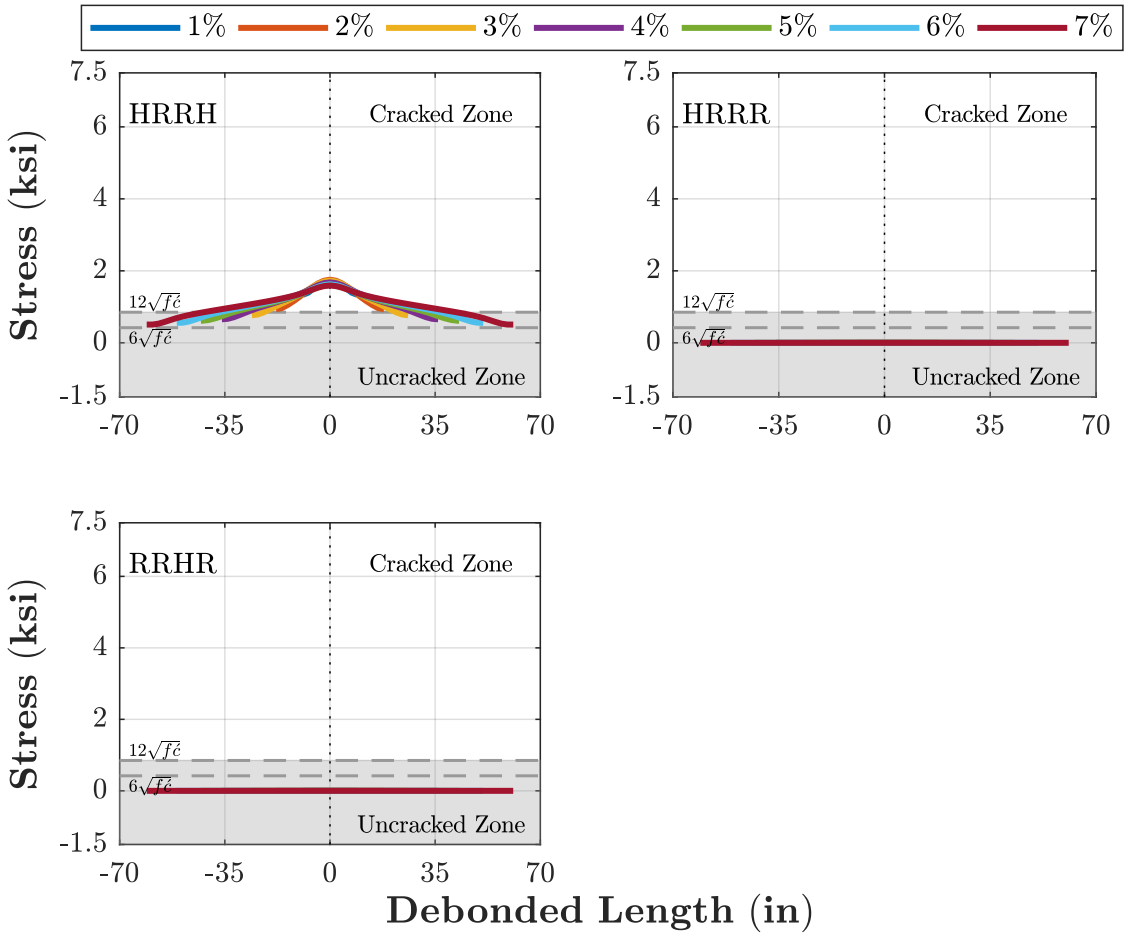

Figure 4.10: Effect of debonding under uniform temperature load for support conditions: HRRH; HRRR; and RRHR

4.3 Conclusions of Parametric Study

It can be concluded from this preliminary analysis that support conditions affect the behavior of link slabs and therefore their effect cannot be neglected. Temperature causes cracking and it can be as severe as that as produced by the live load. For the two loading cases considered in this study, the stresses at the top of the link slab overcome the cracking limit stress for normal concrete (i.e., ranging between 0.42 to 0.85 ksi).

Chapter 5

Findings, Conclusions, and Proposed Recommendations for Implementation

5.1 Summary

The findings, conclusions, and proposed recommendations for implementations are presented in this chapter for each of the three main tasks of the study of Literature Review (Chapter 2); Analysis of Indiana Bridge (Chapter 3); and Bridge Parameter Investigation (Chapter 4). Suggestions for future research are also presented.

5.2 Findings

5.2.1 Literature Review

The literature review conducted in Chapter 2 on the state of practice about link slabs included: (1) State Departments of Transportation (DOT) experience; (2) previous research studies; (3) design specifications and construction practices; and (4) Indiana DOT implementation experience. The salient findings are:

5.2.1.1 State Department of Transportation Experience

(a) Approximately 30% had experience with the use of link slabs, and approximately two-thirds of the reported agencies had performed research or implemented the link-slab system in the field.

(b) The reported cases of implementation of link slabs were mainly in the rehabilitation of steel girder bridge superstructure. In most cases, the link slabs were debonded from the

end girders.

(c) One-third of the agencies having reported experience with the system had design provisions or standard details. Several link slab joint details and materials have been developed and used in the field. However, a standardized geometry and detailing has not been achieved across the DOTs. The details used in link slabs are described in Section 5.2.1.2(b). North Carolina, Michigan, Virginia, and New York were identified as key DOTs in the use of link slabs.

(d) The performance of link slabs implemented so far, varies among transportation agencies. For example, Michigan reported performance varying widely from very good to poor. Cracking was reported as the main issue of link slabs. The cracking was attributed to poor construction practices and improper detailing. There are other agencies such as Virginia, New York, and Massachusetts that have experienced good performance with link slabs. No cracking issues were reported.

(e) Material used in the link slab is another aspect that varies among DOTs. North Carolina and Massachusetts use conventional concrete, while other transportation agencies like Michigan, Virginia, and New York prefer to use fiber reinforced concrete for link slabs applications.

5.2.1.2 Previous Research

Previous research studies showed the focus to be on development more durable materials for use in link slabs. While few studies addressed improvements on design and detailing standards. The salient findings from this portion of the literature review are:

(a) Material: four advanced concrete materials for link slabs have been reported: latex modified concrete (LMC), fiber-reinforced engineering cementitious composite (ECC), ultra-high performance concrete (UHPC), and hybrid fiber-reinforced concrete (HyFRC). Common features between these materials are higher tensile strength and lower permeability. Research by Fu and Zhu [2017] identified ECC and UHPC mixtures as promising candidate options for use in link slabs. The compositions used are described in Section 2.5. Hoomes et al. [2017] showed HyFRC with synthetic fibers provided the most economical solution for crack control and bond strength [See Section 2.2.3]. An alternative to traditional epoxy-coated reinforcement is glass fiber reinforced polymer (GFPR) bars.

(b) Types: three different types of link slabs were identified in the literature: haunched, flexible, and debonded.

i. The haunched and flexible configurations were used in Canada for deck rehabilitation. However, the use has been discontinued due to high costs as well as limitations in the girder end-rotations and girder depth [Lam, 2011].

ii. Currently, the debonded link slab detail is the most commonly used in the United States and Canada. It is described in detail Section 2.2. Four debonded configurations were reported: two full-depth cast-in-place, one partial-depth cast-in-place, and one partial-depth precast. The two full-depth link slabs as well as the one partial-depth cast-in-place have been tested and implemented in the field. The partial-depth precast link slab has been tested but not used in the field.

iii. The first configuration of a full-depth cast-in-place link slab was proposed by Caner and Zia [1998]. The link slab had a debonded zone equivalent to 5% of each adjacent bridge span. The continuity for live load provided by the link slab is neglected. A field inspection conducted by Aktan et al. [2008] on bridges in Michigan indicated full-depth transverse cracks of width between 0.01 to 0.02 in at the centerline on the link slabs using this detail.

iv. The second full-depth cast-in-place link slab configuration was proposed by Li et al. [2003] to address the interfacial cracking problem with the link slab detailing proposed by Caner and Zia [1998]. The Caner and Zia [1998] detail caused by high-stress concentrations at the interface between the link slab and the existing concrete deck. The new detail had a transition zone of 2.5% at each adjacent span in addition to the debonded zone of 5%. This transition zone served to move the interface away from the start point of the debonding. The new detail provides continuity for live load. Testing of this design detail with ECC material and 2.5% debonding under cyclic loading (100,000 cycles) resulted in crack widths less than 0.002 in. while for a link slab using conventional concrete was 0.025 in. No cracks were observed at the interface between the existing deck and the link slab. Li et al. [2005] implemented the new detail in an actual structure in Michigan. The study concluded that ECC link slabs performed as designed. However, shrinkage cracking was reported after three days casting. Crack widths ranged between 0.005 in to 0.014 in. Li et al. [2008] investigated causes of the cracking and recommended limiting skew angle no more than 25 degrees, night casting, and water curing for at least 7 days. The use of stay-in-place forms, and the placement of sidewalk and barrier wall directly over the link slabs was not recommended due to stress concentrations. A transverse saw cut was not also recommended.

v. Partial-depth cast-in-place link slab was used to rehabilitate the SR962G bridge over US Route 17 in Owego, New York. The bridge rehabilitation project involved the use of precast concrete deck panels. The filler material used in the connection was UHPC.

vi. Partial-depth precast link slab details were proposed and tested by Reyes and Robertson [2011] and Larusson et al. [2013]. The details were constructed using ECC reinforced with GFPR bars and tested under tension and compression loads.

(c) Key Performance Factors:

i **Temperature gradients:** Research conducted by Aktan et al. [2008], using design detail by Caner and Zia [1998], concluded that cracks in the link slabs are due mainly to hydration thermal loads and drying shrinkage. The authors recommended to consider thermal loads into the design of link slabs as well as develop new concrete materials that can tolerate these thermal loads. The authors also recommended to use continuous top and bottom reinforcement and provide saw cuts at the ends of the link slab and directly over the pier centerline.

ii **Support conditions:** Caner and Zia [1998] concluded that support conditions do not affect the behavior of link slabs since the measured reactions, strains, and deflections remained the same for all support cases in the elastic range. The measured reactions and load-deflection curves of the girders indicated that each individual span behaved as if it was simply-supported.
Numerical analysis by Ulku et al. [2009] reported a moment value of 50 kip-ft under live and temperature gradient load for support arrangements Hinge-Roller-Roller-Roller and Roller-Roller-Hinge-Roller. A reduced moment value of 19 kip-ft with increased axial force was reported for Roller-Hinge-Hinge-Roller case.

iii **Length of debonding:** Numerical analysis performed by El-Safty and Okeil [2008] showed that a debonded length of 5% increases the load-carrying capacity of the beam by about 11.6% when compared to that of an unbonded beam.
Ulku et al. [2009] observed that link slab moment decreases with increasing the debonded length but remains constant after a debonding of 5%. No changes in the net axial force were observed when varying the debonded length since the axial stiffness of the link slab remained constant.

5.2.1.3 Design Specifications and Construction Practices

To date, there is no national survey of highway agencies that documents the state of practice on link slabs. The review of the specifications and the proposed AASHTO guidelines for accelerated bridge construction reveals that the majority of the states use:

(a) The design methodology proposed by Caner and Zia [1998] in North Carolina. Accordingly, the girder end rotation due to live load and the AASHTO crack limit are used as design criteria. It must be noted that none of the states consider thermal effects in the design of the link slab.

(b) A debonded length of 5% to 7% at each span. No transition zone is specified by the states.

(c) Full-depth link slabs. Only the state of New York indicates the use of a partial-depth configuration.

(d) Specify a 7-day wet curing period.

(e) Only three agencies, North Carolina, Virginia, and Florida specify maximum span length. The corresponding lengths are 75 ft, 100 ft, and 100 ft.

(f) Specified concrete materials by North Carolina, Virginia, and New York are Class AA Concrete, Low Shrinkage Class A4 Modified Concrete, and UHPC, respectively.

5.2.1.4 Indiana DOT Implementation Experience

The findings discussed in this section are based on the study of the inspection reports and the drawings of the bridges analyzed in Indiana. Unfortunately, the inspection reports reviewed lack more numerical data to allow in-depth analysis of the behavior of the link slab bridges. These reports are based only on subjective visual inspections with no exact data of crack parameters like exact locations, width, and depth. The following findings are observed:

(a) Most link slab construction is recent with no enough inspection reports after the construction to observe the bridge performance in the long term. All analyzed link slab bridges were constructed in the years 2013 to 2017 with a maximum of two inspection reports post link slab construction.

(b) All reviewed bridges in Indiana had the link slabs constructed as part of the rehabilitation.

(c) Link slabs mostly follow the haunched type detail, i.e., deeper than the deck (see Chapter 2). In this detail, the link slab is fully bonded to the adjacent slabs as well as the girders with no debonding.

(d) Six link slab bridges included approach slabs constructed alongside the construction of link slabs during the rehabilitation of the bridges out of the seven reviewed. Approach slabs eliminate the possibility of the deck expansion over the abutments.

(e) All link slabs analyzed including one with debonded detail were constructed using conventional normal strength Class C concrete.

(f) All analyzed bridges except the one with debonded link slab detail experienced deterioration and cracking after the link slab construction. Cracking patterns and locations vary throughout the bridges.

(g) Although the inspection reports are recent, most analyzed Indiana bridges experienced cracking within the first year of the link slab construction.

(h) In addition to the various cracking patterns, transverse cracking of the deck in the vicinity of the link slabs is common in most bridges after the link slab construction. The transverse cracking is more evident and stronger in decks supported by steel girders.

5.2.2 Analysis of Indiana Bridge

The bridge (#68-65-5213A) crossing the State Road 68 over the Interstate 64 was modeled numerically to evaluate the bridge performance after the construction of link slabs numerically in Chapter 3. Two models were analyzed to represent the bridge superstructure prior to the link slabs construction (i.e., including expansion joints) and compare with the bridge superstructure post link slab construction (i.e., jointless deck) subjected to both live loads and thermal loads. The link slab detail implemented in this bridge was the haunched type detail. The results indicated that the critical action of the superstructure was the longitudinal axial stress in the concrete deck. Therefore, only these stresses are presented in this section and, for simplicity, will be referred to as stresses. These findings of the numerical analysis are described in reference to solicitation, type of superstructure, and bridge support conditions:

(a) Live load: the analysis showed that the presence of the link slab in replacement of the longitudinal joints reduced compressive stresses at midspan of the deck as a result of the continuity provided by the link slab. On the other hand, the link slabs themselves experienced tensile stresses that can be maximized by fully loading the adjacent spans.

(b) Thermal loads: two types of thermal loadings were considered, gradient and uniform. Gradient temperature loading induced compressive stresses in the link slabs. The magnitude of the stresses was almost 50% of the magnitude of stresses induced due to live loads. However, a uniform decrease in temperature induced tensile stresses in the link slab, while a uniform increase in temperature induced compressive stresses. Prior to installation of the link slab, for purposes of comparison, the model was built with expansion joints. It was shown that the maximum longitudinal stresses in the deck slab of the bridge with uniform temperature loading occurred at the bridge intermediate pier connecting the continuous steel spans. The model with the link slab and existing boundary conditions indicated that maximum stresses in the deck slab due to uniform temperature loading occurred at the link slabs. The magnitude of these stresses was around 3.5 times the maximum on the deck at that location prior to installing the link slab. However, the stresses due to uniform temperature loading over the intermediate pier connecting the two continuous steel spans were the same with both models.

(c) Effect of bridge superstructure Type: to better understand the behavior of link slabs, a new model was developed by replacing the existing steel girders with concrete ones after the link slab is installed and referred to as concrete model. The model was selected to test if the observed thermal stresses in the model of the existing bridge can be attributed to the difference in expansion between the steel girders and concrete deck. Similar to the original model, the controlling actions on the superstructure were the longitudinal axial stresses in the deck. The magnitude of the maximum stresses due to uniform temperature loading in the concrete model was twice the same stresses in the original bridge prior to the link slab installment. Similar to the original bridge once the link slab was in place, the distribution of the axial stresses in the deck was almost constant throughout the intermediate two spans in the concrete model; and the maximum stresses in the concrete model due to uniform temperature loading were 1.6 times the maximum stresses prior to installation of the link slab. The stresses in the link slabs in either the original model post link slab or the concrete bridge due to live loads were 1.4 times the cracking stress of the normal strength concrete, while the same stresses due to uniform decrease in temperature were at least four times the cracking stress.

(d) Bridge support conditions: since the support conditions have been reported to influence the link slab performance in bridges, three variations on the original model with link slab construction were studied to compare the effect on the longitudinal stresses in the deck. The stresses in the link slabs due to live loads decreased with less restraints at the girders supports. The model simulating all roller supports had lower stresses in the link slabs, while the existing bridge model which included fixed supports had the highest stresses in the link slabs. Live load stresses at midspan of the intermediate steel spans increased when reducing the restraints; and, did not change significantly among the models with different boundary conditions at the continuous steel spans with the exception of the all-rollers model with a uniform decrease in temperature. Stresses due to uniform decrease in temperature in the deck of the concrete spans in the approach slab model were twice as much as those stresses in the all-rollers model. Stresses due to any temperature loading case were almost zero in the all-rollers model.

5.2.3 Bridge Parameter Investigation

In Chapter 4, to further extend the analysis observations from the study in the Indiana bridge conducted in Chapter 3, a series of 3D finite element models were developed to evaluate the effect of support conditions and debonded length on the longitudinal stress distribution in the deck and potential crack initiation in link slabs. Two bridge structures were investigated. The first structure (Case 1) represented a bridge structure rehabilitated using link slabs. The second bridge structure (Case 2) had same geometrical and material properties as Case 1, but the concrete deck was continuous and fully bonded. The girder boundary conditions

were defined as combinations of Fixed (F), Hinged (H), and Roller (R) support. The findings describe the bridge in that fashion and are presented in terms of longitudinal normal stresses measured at the top layer of the link slabs. All findings discussed in this section are limited to the range of parameters considered in Chapter 4.

(a) Effect of girder support conditions: for the configurations RRHR, HRRH, FFRH, and HRHH, allowing horizontal movement at interior supports leads to an increase in the magnitude of normal stresses in the link slab under live load. Stresses were three times greater than the cracking limit stress for normal concrete. Due to symmetry in the model, stresses in the link slabs remained the same when having fixed (i.e., FFRH) or pinned supports at the ends (i.e., HRHH) under the live loading cases considered. Stresses in the link slab due to live load were approximately three times greater than those observed due to temperature loads for all boundary conditions considered (i.e., FFRH, HHHH, HRHH, HRRH, HRRR, RHHR, RRHR). Change position of hinge (H) support location in the configurations HRRR and RRHR did not produce any difference on the link slab stresses under both live and thermal loads.

(b) Effect of debonded length: 5% of the span length as debonded length reduced stresses due to live load around 38% compared with the continuous and fully bonded deck. Debonding reduced stresses due to live load with an optimum length of around 5% to 6%.

5.3 Conclusions

From the findings in the literature review and numerical studies, the following conclusions, identified by subject, can be drawn:

5.3.1 Use by DOTs

(a) Link slabs have been used for rehabilitation purposes in steel girder bridge superstructure. The majority of the cases where the link slab has been implemented consisted of debonded full-depth link slabs except for Indiana and New York as recommended in the Caner and Zia [1998] study. In Indiana, fully bonded and full-depth link slabs were used, and in New York with partial depth and debonded link slabs.

(b) With respect to the material of the link slab, North Carolina, Indiana and Massachusetts used normal strength concrete, while Michigan, Virginia and New York used low permeability higher tensile strength concrete with steel fibers.

(c) North Carolina, Michigan, Virginia, and New York are the states report more use of link slabs.

(d) The presence of a transition zone into the existing deck beyond the debonded length of the link slab has been investigated and implemented by Michigan with mixed performance. In the laboratory showed good performance with respect to cracking while in the field the implementation experienced cracking in the link slab.

(e) To date thermal loading is not considered in the design of link slabs.

5.3.2 Design Practice

Current design approach for link slabs includes simply supported girder end rotation [Caner and Zia, 1998] in conjunction with AASHTO crack width limitation [AASHTO, 2017]. The thermal effects although mentioned in research studies, are not considered in practice by the DOTs responded in this study.

Additional conclusions from the findings from analytical and research studies indicate that:

(a) The construction of the approach slabs alongside the link slabs construction restrains the bridge against thermal expansion causing high stresses due to thermal loads. The effect of uniform thermal loads on the bridge superstructure including the existing deck and the link slabs is highly dependent on the type of the superstructure girders whether concrete or steel girders and their support conditions. The identification of this effect come from limited research studies.

(b) Debonding length of 5% is the optimum debonding length to induce the minimum longitudinal tensile stresses in the link slabs due to live loads.

(c) Use of higher tensile strength and low permeability concrete materials are recommended in the construction of link slabs.

(d) Effective strategies to minimize cracking reported in the literature are night-time casting, adequate curing, and the use of continuous top and bottom reinforcement.

5.3.3 Research

A few gaps have been identified during the current study where more research is recommended.

(a) The literature and analysis results show the influence of girder end support conditions on link slab stresses. A link slab over RHHR support configuration is subjected to both axial forces and flexure. However, this combined effect is not considered in the current design methodology for link slabs.

(b) Research has focused on development more durable materials for use in link slabs. Few studies addressed improvements on design and detailing standards, and there is a paucity of data on the performance of precast concrete link slabs.

(c) The modified Caner and Zia proposed design detail was modified in a subsequent study by adding a transition zone and ECC material. This detail was shown to have satisfactory performance in the laboratory under both cyclic and ultimate loads. No deterioration was observed at the interface between the existing deck and the link slab. However, in the field implementation early shrinkage and possibly temperature cracking was observed. Further evaluation of this detail in the lab and the field is recommended as the most promising form of construction for the link slabs.

(d) Promising materials recommended in the literature for use in link slabs, listed in order of reported successful performance, are:

  (i) ultra-high performance concrete (UHPC) and fiber-reinforced engineering cementitious composite (ECC).

  (ii) hybrid fiber-reinforced concrete (HyFRC) is suggested as an economical solution compared to the UHPC and ECC mixtures. However, this material has not been implemented in the field.

5.4 Recommendations for Implementation

Based on the conclusions from the study, the following recommendations are presented for consideration and possible implementation.

(a) It is recommended to use 5% debonding length and link slab detailing recommended by Caner and Zia [1998], with the additional transition zone into the existing deck (Fig. 5.1), to minimize the overall longitudinal tensile stresses in the link slabs. Laboratory studies conducted by Li et al. [2003] showed that the introduction of the transition zone eliminated cracking due to loads at the interface of the debonded link slab. It is recommended to investigate improved reinforcement details and material specifications to address construction issues and enhance long-term performance.

(b) Since, in almost all cases studied, link slabs see high tensile stresses that are higher than the cracking limit of conventional normal-strength concrete, it is recommended to use high tensile materials for the link slabs. The literature addresses this issue extensively and provide better alternatives such as UHPC, ECC, and FRP. However, the use of these materials alone may not guarantee un-cracked link slabs without further consideration of thermal loading and the detailing of the link slab.

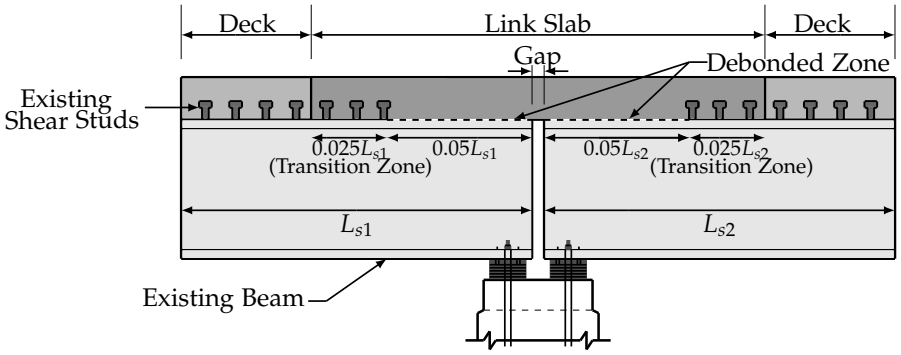

Figure 5.1: ECC link slab configuration proposed by Li et al. [2003]

(c) Allowing thermal expansion of the bridge could reduce the possibility of cracking due to all thermal loads, has high potential of therefore reducing the cracking and deterioration of the bridges with link slab construction.

(d) Currently, there is limited information that allows to identify and evaluate the key factors affecting the performance of the existing bridges in Indiana. More detailed inspections on link slab bridges are recommended to include parameters such as crack width, depth, and mapping of crack locations together with long-term evaluation.

(e) The simplified equations used in literature to analyze link slabs are not accurate or conservative enough to serve as a sole base for design. It is recommended to analyze the link slab more thoroughly with more sophisticated tools such as FE analysis until a reliable simplified method is developed.

(f) The variability in link slab details tested by researchers presents a great difficulty in objectively assessing the comparative performance of the different materials and details used. It is recommended to have a unified testing standard for link slabs that is able to mimic the real link slab performance in the field.

5.5 Suggestions for Future Research

The authors recommend further investigation on improved analysis methods that properly take into account the effect of temperature loads and support conditions as well as the advanced material properties. Laboratory testing and actual field demonstration are also needed to evaluate the performance of the recommended design detail and materials.

References

AASHTO (2017). Bridge design specifications and commentary. In *AASHTO LRFD*. American Association of State Highway and Transportation Officials, Washington, DC.

Aktan, H. and Attanayake, U. (2011). High skew link slab bridge system with deck sliding over backwall or backwall sliding over abutments. Report. No. RC-1563, Michigan Department of Transportation, Lansing, MI.

Aktan, H., Attanayake, U., and Ulku, E. (2008). Combining link slab, deck sliding over backwall, and revising bearings. Report. No. RC-1514, Michigan Department of Transportation, Kalamazoo, MI.

Alampalli, S. and Yannotti, A. (1998). In-Service Performance of Integral Bridges and Jointless Decks. *Transportation Research Record: Journal of the Transportation Research Board*, 1624(98-0540):1–7.

Au, A., Lam, C., Au, J., and Tharmabala, B. (2013). Eliminating Deck Joints Using Debonded Link Slabs : Research and Field Tests in Ontario. *Journal of Bridge Engineering*, 18(8):768–778.

Caner, A., Dogan, E., and Zia, P. (2002). Seismic Performance of Multisimple-Span Bridges Retrofitted with Link Slabs. *Journal of Bridge Engineering*, 7(2):85–93.

Caner, A. and Zia, P. (1998). Behavior and Design of Link Slabs for Jointless Bridge Decks. *PCI Journal*, 43(3):68–80.

Culmo, M. P., Marsh, L., and Stanton, J. (2017). Recommended aashto guide specifications for abc design and construction. Final Report for Project 12-102, National Cooperative Highway Research Program, Transportation Research Board, Washington, D.C.

El-Safty, A. (1994). *Behavior of Jointless Bridge Decks*. PhD thesis, North Carolina State University, Raleigh, NC.

El-Safty, A. and Okeil, A. (2008). Extending the Service Life of Bridges using Continuous Decks. *PCI Journal*, 53(6):96–111.

FDOT (2018). Bridge maintenance course series—reference manual. In *Bridge Division*. Florida Department of Transportation, Tallahassee, FL.

Fu, C. C. and Zhu, Y. F. (2017). A pilot application of link slab with selected material for mdta steel bridges. Technical report, Maryland Transportation Authority, Baltimore, MD.

Gastal, F. (1986). *Instantaneous and Time-Dependent Response and Strength of Jointless Bridge Beams*. PhD thesis, North Carolina State University, Raleigh, NC.

Gastal, F., and Zia, P. (1989). Analysis of bridge beams with jointless decks. In *International Association for Bridge and Structural Engineering (IABSE)*, pages 555–560.

Graybeal, B. (2014). Design and construction of field-cast uhpc connections. Final Report. No. FHWA-HRT-14-084, Office of Infrastructure Research and Development, McLean, VA.

Hoomes, L., Ozyildirim, H. C., and Brown, M. (2017). Evaluation of high-performance fiber-reinforced concrete for bridge deck connections, closure pours, and joints. Final Report. No. FHWA-VTRC-17-R15, Virginia Transportation Research Council, Charlottesville, VA.

Hou, M., Hu, K., Yu, J., Dong, S., and Xu, S. (2018). Experimental Study on Ultra-High Ductility Cementitious Composites Applied to Link Slabs for Jointless Bridge Decks. *Composite Structures*, 204(2018):167–177.

Kim, Y., Fischer, G., and Li, V. C. (2004). Performance of Bridge Deck Link Slabs Designed with Ductile Engineered Cementitious Composite. *ACI Structural Journal*, 101(6):792–801.

Lam, C. (2011). Pulling the Teeth on Old Bridge Structures Eliminating Bridge Expansion Joints with Concrete Link Slabs. *Ontario's Transportation Technology Transfer Digest Road Talk*, 1(Article 8):1–3.

Lam, C., Lai, D., Au, J., Lim, L., Young, W., and Tharmabala, B. (2008). Development of Concrete Link Slabs to Eliminate Bridge Expansion Joints over Piers. *Annual Conference of the Transportation Association of Canada*, pages 1–20.

Larusson, L., Reyes, J., Lum, B., Fischer, G., and Robertson, I. N. (2013). Development of flexible link slabs using ductile fiber reinforced concrete. Final Report. No. UHM-CEE-13-04, Hawaii Department of Transportation, Honolulu, HI.

Lepech, M. D. and Li, V. C. (2008). Large-Scale Processing of Engineered Cementitious Composites. *ACI Materials Journal*, 105(4):358–366.

Lepech, M. D. and Li, V. C. (2009). Application of ECC for bridge deck link slabs. *Materials and Structures*, 2009(42):1185–1195.

Li, G. and Saber, A. (2009). Elimination of deck joints using a corrosion resistant frp approach. Final Report. No. FHWA-LA-09-443, Louisiana Department of Transportation and Development, Baton Rouge, LA.

Li, V., Fischer, G., Kim, Y., Lepech, M., Qian, S., Weimann, M., and Wang, S. (2003). Durable link slabs for jointless bridge decks based on strain-hardening cementitious composites. Report. No. RC-1438, Michigan Department of Transportation, Lansing, MI.

Li, V., Lepech, M., and Li, M. (2005). Field demonstration of durable link slabs for jointless bridge decks based on strain-hardening cementitious composites. Report. No. RC-1471, Michigan Department of Transportation, Lansing, MI.

Li, V., Yang, E., and Li, M. (2008). Field demonstration of durable link slabs for jointless bridge decks based on strain-hardening cementitious composites-phase 3: Shrinkage control. Report. No. RC-1506, Michigan Department of Transportation, Lansing, MI.

MassDOT (2013). Lrfd bridge manual - part i. In *Highway Division*. Massachusetts Department of Transportation, Boston, MA.

NCDOT (2018). Structures management unit manual. In *Contract Standards and Development Unit*. North Carolina Department of Transportation, Raleigh, NC.

NYSDOT (2018). Bridge manual. In *Engineering Division*. New York State Department of Transportation, Richmond, VA.

Okeil, A. and El-Safty, A. (2005). Partial Continuity in Bridge Girders with Jointless Decks. *Practice Periodical on Structural Design and Construction*, 10(4):229–238.

Ozyildirim, H. C., Khakimova, E., Nair, H., and Moruza, G. M. (2017). Fiber-Reinforced Concrete in Closure Pours over Piers. *ACI Materials Journal*, 114(3):397–406.

PCI (1992). In *PCI Design Handbook*. Precast/Prestressed Concrete Institute, Chicago, IL.

Reyes, J. and Robertson, I. N. (2011). Precast link slab for jointless bridges decks. Final Report. No. UHM-CEE-11-09, Hawaii Department of Transportation, Honolulu, HI.

Royce (2016). Utilization of Ultra-High Performance Concrete (UHPC) in New York. In *First International Interactive Symposium on UHPC*, pages 1–9.

Sevgili, G. and Caner, A. (2009). Improved Seismic Response of Multisimple-Span Skewed Bridges Retrofitted with Link Slabs. *Journal of Bridge Engineering*, 14(6):452–459.

UDOT (2017). Structures design and detailing manual. In *Highway Division*. Utah Department of Transportation, Salt Lake City, UT.

Ulku, E., Attanayake, U., and Aktan, H. (2009). Jointless Bridge Deck with Link Slabs Design for Durability. *Transportation Research Record: Journal of the Transportation Research Board*, 1(2131):68–78.

VDOT (2016a). Vdot road and bridge specifications. In *Structure and Bridge Division*. Virginia Department of Transportation, Richmond, VA.

VDOT (2016b). Vdot supplement to the aashto manual for bridge element inspection. In *Structure and Bridge Division*. Virginia Department of Transportation, Richmond, VA.

VDOT (2018). Manual of the structure and bridge division. In *Part 2 Design Aids and Typical Details*. Virginia Department of Transportation, Richmond, VA.

Wing, K. M. and Kowalsky, M. J. (2005). Behavior , Analysis , and Design of an Instrumented Link Slab Bridge. *Journal of Bridge Engineering*, 10(3):331–344.

Zheng, Y., Zhang, L., and Xia, L. (2018). Investigation of the Behaviour of Flexible and Ductile ECC Link Slab Reinforced with FRP. *Construction and Building Materials*, 166(2018):694–711.

About the Joint Transportation Research Program (JTRP)

On March 11, 1937, the Indiana Legislature passed an act which authorized the Indiana State Highway Commission to cooperate with and assist Purdue University in developing the best methods of improving and maintaining the highways of the state and the respective counties thereof. That collaborative effort was called the Joint Highway Research Project (JHRP). In 1997 the collaborative venture was renamed as the Joint Transportation Research Program (JTRP) to reflect the state and national efforts to integrate the management and operation of various transportation modes.

The first studies of JHRP were concerned with Test Road No. 1—evaluation of the weathering characteristics of stabilized materials. After World War II, the JHRP program grew substantially and was regularly producing technical reports. Over 1,600 technical reports are now available, published as part of the JHRP and subsequently JTRP collaborative venture between Purdue University and what is now the Indiana Department of Transportation.

Free online access to all reports is provided through a unique collaboration between JTRP and Purdue Libraries. These are available at: http://docs.lib.purdue.edu/jtrp

Further information about JTRP and its current research program is available at: http://www.purdue.edu/jtrp

About This Report

An open access version of this publication is available online. See the URL in the recommended citation below.

Haikal, G., Ramirez, J. A., Jahanshahi, M. R., Villamizar, S., & Abdelaleim, O. (2019). *Link slab details and materials* (Joint Transportation Research Program Publication No. FHWA/IN/JTRP-2019/10). West Lafayette, IN: Purdue University. https://doi.org/10.5703/1288284316920